List of tables in main document.

Table 1. Managed recharge volumes for eastern Snake River Plain.
Table 2. Start and end dates for model stress periods.
Table 3. River cells used in ESPAM.
Table 4. Drain cells used in ESPAM.
Table 5. List of tributary basins.
Table 6. List of perched reaches.
Table 7. List of canal cells.
Table 8. Measured lysimeter winter ET.
Table 9. Estimated winter ET by weather station.
Table 10. Irrigation entity table.
Table 11. Irrigation interpolation points for migration to sprinkler.
Table 12. Measured return flow sites.
Table 13. Assignment of return flow sites to irrigation entities.
Table 14. Table of return flow lags for the ten groups of irrigation entities.
Table 15. Normalized Silver Creek annual flows.
Table 16. Minor land-use types for non-irrigated recharge estimation.
Table 17. Apportionment of Mud Lake fixed pumping.
Table 18. Summary of fixed pumping rates by stress period for each class of fixed pumping well.
Table 19. Evapotranspiration-indexed scale used to vary off-site pumping rates.
Table 20. Off-site well pumping for each model stress period.
Table 21. Annual spring discharge (north side only) in the Milner to King Hill reach.
Table 22. Estimated spring discharge by sub-reach in the Milner to King Hill reach.
Table 23. Model cells representing individually measured or estimated springs.
Table 24. Summary of spring discharge calibration target data.
Table 25. Steady state river gain and spring calibration targets and model predictions.
Table 26. ESPAM Design Document list.

Table 1. Managed recharge volumes for eastern Snake River Plain.

Year	Volume (ac-ft)
1995	180,000
1996	169,000
1997	230,000
1998	201,000
1999	153,000
2000	70,000
2001 and later	none

Table 2. Start and end date for model stress periods. Irrigation season stress periods start on May 1 and end on October 31 of the same year. Non-irrigation season stress periods start on November 1 and end on April 30 of the following year.

Period	Start Month	End Month	Length (days)	Period	Start Month	End Month	Length (days)
SP001	May, 1980	Oct, 1980	182	SP023	May, 1991	Oct, 1991	182
SP002	Nov, 1980	April, 1981	183	SP024	Nov, 1991	April, 1992	183
SP003	May, 1981	Oct, 1981	182	SP025	May, 1992	Oct, 1992	182
SP004	Nov, 1981	April, 1982	183	SP026	Nov, 1992	April, 1993	183
SP005	May, 1982	Oct, 1982	182	SP027	May, 1993	Oct, 1993	182
SP006	Nov, 1982	April, 1983	183	SP028	Nov, 1993	April, 1994	183
SP007	May,1983	Oct, 1983	182	SP029	May, 1994	Oct, 1994	182
SP008	Nov, 1983	April, 1984	183	SP030	Nov, 1994	April, 1995	183
SP009	May, 1984	Oct, 1984	182	SP031	May, 1995	Oct, 1995	182
SP010	Nov, 1984	April, 1985	183	SP032	Nov, 1995	April, 1996	183
SP011	May, 1985	Oct, 1985	182	SP033	May, 1996	Oct, 1996	182
SP012	Nov, 1985	April, 1986	183	SP034	Nov, 1996	April, 1997	183
SP013	May, 1986	Oct, 1986	182	SP035	May, 1997	Oct, 1997	182
SP014	Nov, 1986	April, 1987	183	SP036	Nov, 1997	April, 1998	183
SP015	May, 1987	Oct, 1987	182	SP037	May, 1998.	Oct, 1998	182
SP016	Nov, 1987	April, 1988	183	SP038	Nov, 1998	April, 1999	183
SP017	May, 1988	Oct, 1988	182	SP039	May, 1999	Oct, 1999	182
SP018	Nov, 1988	April, 1989	183	SP040	Nov, 1999	April, 2000	183
SP019	May, 1989	Oct, 1989	182	SP041	May, 2000	Oct, 2000	182
SP020	Nov, 1989	April, 1990	183	SP042	Nov, 2000	April, 2001	183
SP021	May, 1990	Oct, 1990	182	SP043	May, 2001	Oct, 2001	182
SP022	Nov, 1990	April, 1991	183	SP044	Nov, 2001	April, 2002	183

Table 3. List of model cells containing river cells representing the Snake River.

Row	Column	Stage (ft)	Riverbed Conductance (ft^2/day)	River Bottom Elevation (ft)	Reach
52	200	5059.56	1.01E+06	5020.45	Ashton to Rexburg
52	201	5072.45	1.01E+06	5034.25	Ashton to Rexburg
53	197	5018.37	1.01E+06	4977.65	Ashton to Rexburg
53	198	5034.22	1.01E+06	4993.48	Ashton to Rexburg
53	199	5045.92	1.01E+06	5005.63	Ashton to Rexburg
54	182	4826.99	1.01E+06	4790.52	Ashton to Rexburg
54	183	4828.79	1.01E+06	4792.48	Ashton to Rexburg
54	184	4836.26	1.01E+06	4800.14	Ashton to Rexburg
54	185	4840.07	1.01E+06	4803.99	Ashton to Rexburg
54	186	4848.72	1.01E+06	4812.76	Ashton to Rexburg
54	187	4859.43	1.01E+06	4823.79	Ashton to Rexburg
54	188	4866.33	1.01E+06	4831.1	Ashton to Rexburg
54	189	4876.77	1.01E+06	4842.16	Ashton to Rexburg
54	190	4901.92	1.01E+06	4867.95	Ashton to Rexburg
54	191	4914.41	1.01E+06	4880.7	Ashton to Rexburg
54	192	4945.66	1.01E+06	4912.51	Ashton to Rexburg
54	193	4963.37	1.01E+06	4928.95	Ashton to Rexburg
54	194	4980.06	1.01E+06	4942.81	Ashton to Rexburg
54	195	4994.97	1.01E+06	4954.97	Ashton to Rexburg
54	196	5007.84	1.01E+06	4967.19	Ashton to Rexburg
55	180	4818.69	1.01E+06	4781.67	Ashton to Rexburg
55	181	4823.2	1.01E+06	4786.41	Ashton to Rexburg
56	178	4814.93	1.01E+06	4777.38	Ashton to Rexburg
56	179	4816.46	1.01E+06	4779.12	Ashton to Rexburg
56	168	4770.82	1.10E+05	4730.46	Heise to Shelley
56	169	4775.57	1.10E+05	4735.15	Heise to Shelley
56	170	4779.76	1.10E+05	4739.28	Heise to Shelley
57	166	4763.71	1.10E+05	4723.57	Heise to Shelley
57	167	4766.42	1.10E+05	4726.23	Heise to Shelley
57	170	4784.37	1.10E+05	4743.82	Heise to Shelley
57	177	4813.42	1.10E+05	4775.62	Heise to Shelley
58	166	4764.36	1.10E+05	4724.34	Heise to Shelley
58	167	4764.85	1.10E+05	4724.8	Heise to Shelley
58	171	4790.95	1.10E+05	4750.3	Heise to Shelley
58	174	4807.07	1.10E+05	4766.88	Heise to Shelley
58	175	4809.3	1.10E+05	4769.74	Heise to Shelley
58	176	4810.94	1.10E+05	4772.55	Heise to Shelley
59	165	4762.48	1.10E+05	4722.56	Heise to Shelley
59	166	4764.36	1.10E+05	4724.4	Heise to Shelley
59	171	4794.72	1.10E+05	4754.03	Heise to Shelley
59	174	4807.5	1.10E+05	4774.5	Heise to Shelley
60	164	4759.23	1.10E+05	4719.36	Heise to Shelley
60	172	4797.76	1.10E+05	4757.04	Heise to Shelley

Table 3 (contd.). List of model cells containing river cells representing the Snake River.

Row	Column	Stage (ft)	Riverbed Conductance (ft^2/day)	River Bottom Elevation (ft)	Reach
60	173	4802.84	1.10E+05	4762.07	Heise to Shelley
60	174	4811.5	1.10E+05	4778.5	Heise to Shelley
61	164	4758.28	1.10E+05	4718.46	Heise to Shelley
61	175	4830	1.10E+05	4797	Heise to Shelley
62	164	4755.48	1.10E+05	4715.76	Heise to Shelley
62	175	4837.5	1.10E+05	4804.5	Heise to Shelley
63	164	4753.39	1.10E+05	4713.72	Heise to Shelley
63	175	4844.5	1.10E+05	4811.5	Heise to Shelley
64	164	4749.19	1.10E+05	4709.61	Heise to Shelley
64	176	4865.5	1.10E+05	4832.5	Heise to Shelley
65	164	4744.68	1.10E+05	4705.43	Heise to Shelley
65	176	4873.5	1.10E+05	4840.5	Heise to Shelley
65	177	4884	1.10E+05	4851	Heise to Shelley
66	163	4739.41	1.10E+05	4700.6	Heise to Shelley
66	177	4896.5	1.10E+05	4863.5	Heise to Shelley
67	163	4737.56	1.10E+05	4699.08	Heise to Shelley
67	178	4912.5	1.10E+05	4879.5	Heise to Shelley
68	163	4735.39	1.10E+05	4697.22	Heise to Shelley
68	178	4926.5	1.10E+05	4893.5	Heise to Shelley
69	162	4720.53	1.10E+05	4682.79	Heise to Shelley
69	178	4788.82	1.10E+05	4755.82	Heise to Shelley
70	161	4707.02	1.10E+05	4669.82	Heise to Shelley
70	179	4770.5	1.10E+05	4737.5	Heise to Shelley
71	161	4701.45	1.10E+05	4664.52	Heise to Shelley
71	180	4786	1.10E+05	4753	Heise to Shelley
72	161	4690.55	1.10E+05	4654.02	Heise to Shelley
72	180	4797	1.10E+05	4764	Heise to Shelley
73	160	4677.21	1.10E+05	4641.1	Heise to Shelley
73	180	4809	1.10E+05	4776	Heise to Shelley
74	157	4647.71	1.10E+05	4612.6	Heise to Shelley
74	158	4658.3	1.10E+05	4622.86	Heise to Shelley
74	159	4665.72	1.10E+05	4630.04	Heise to Shelley
74	180	4816	1.10E+05	4783	Heise to Shelley
74	181	4818	1.10E+05	4785	Heise to Shelley
75	153	4606.84	1.10E+05	4572.26	Heise to Shelley
75	156	4629.01	1.10E+05	4594.46	Heise to Shelley
75	181	4818	1.10E+05	4785	Heise to Shelley
76	154	4610.81	1.10E+05	4576.84	Heise to Shelley
76	155	4617.41	1.10E+05	4583.2	Heise to Shelley
76	181	4818	1.10E+05	4785	Heise to Shelley
76	152	4598.48	1.57E+05	4561.11	Shelley to Near Blackfoot
77	151	4589.92	1.57E+05	4548.08	Shelley to Near Blackfoot
77	152	4595.78	1.57E+05	4556.51	Shelley to Near Blackfoot

Table 3 (contd.). List of model cells containing river cells representing the Snake River.

Row	Column	Stage (ft)	Riverbed Conductance (ft^2/day)	River Bottom Elevation (ft)	Reach
78	150	4575.03	1.57E+05	4532.01	Shelley to Near Blackfoot
79	149	4569.54	1.57E+05	4526.38	Shelley to Near Blackfoot
80	147	4553.89	1.57E+05	4510.25	Shelley to Near Blackfoot
80	148	4560.89	1.57E+05	4517.62	Shelley to Near Blackfoot
81	139	4491.97	1.57E+05	4453.9	Shelley to Near Blackfoot
81	140	4501.35	1.57E+05	4461.96	Shelley to Near Blackfoot
81	141	4513.71	1.57E+05	4472.78	Shelley to Near Blackfoot
81	142	4521.68	1.57E+05	4478.88	Shelley to Near Blackfoot
81	143	4527.72	1.57E+05	4484.18	Shelley to Near Blackfoot
81	144	4535.9	1.57E+05	4491.21	Shelley to Near Blackfoot
81	145	4541.93	1.57E+05	4497.1	Shelley to Near Blackfoot
81	146	4547.91	1.57E+05	4503.68	Shelley to Near Blackfoot
82	128	4418.1	1.57E+05	4383.03	Shelley to Near Blackfoot
82	129	4423.53	1.57E+05	4388.8	Shelley to Near Blackfoot
82	130	4431.3	1.57E+05	4396.07	Shelley to Near Blackfoot
82	131	4435.75	1.57E+05	4400.34	Shelley to Near Blackfoot
82	132	4442.82	1.57E+05	4407.11	Shelley to Near Blackfoot
82	133	4448.35	1.57E+05	4412.2	Shelley to Near Blackfoot
82	134	4456.59	1.57E+05	4419.38	Shelley to Near Blackfoot
82	135	4464.03	1.57E+05	4425.76	Shelley to Near Blackfoot
82	136	4472.21	1.57E+05	4433.43	Shelley to Near Blackfoot
82	137	4477.15	1.57E+05	4438.74	Shelley to Near Blackfoot
82	138	4485.21	1.57E+05	4447.49	Shelley to Near Blackfoot
83	127	4408.11	1.57E+05	4372.24	Shelley to Near Blackfoot
83	115	4354.09	9.90E+04	4314.81	Near Blackfoot to Neeley
83	116	4357.37	9.90E+04	4318.34	Near Blackfoot to Neeley
83	126	4402.41	9.90E+04	4365.84	Near Blackfoot to Neeley
84	114	4353.66	9.90E+04	4314.18	Near Blackfoot to Neeley
84	115	4354.09	9.90E+04	4314.81	Near Blackfoot to Neeley
84	116	4357.37	9.90E+04	4318.34	Near Blackfoot to Neeley
84	125	4393.24	9.90E+04	4354.98	Near Blackfoot to Neeley
84	126	4399.29	9.90E+04	4361.92	Near Blackfoot to Neeley
85	112	4353.76	9.90E+04	4313.88	Near Blackfoot to Neeley
85	113	4353.66	9.90E+04	4314.01	Near Blackfoot to Neeley
85	114	4353.66	9.90E+04	4314.18	Near Blackfoot to Neeley
85	115	4354.09	9.90E+04	4314.81	Near Blackfoot to Neeley
85	116	4357.37	9.90E+04	4318.34	Near Blackfoot to Neeley
85	122	4378.63	9.90E+04	4336.98	Near Blackfoot to Neeley
85	123	4382.95	9.90E+04	4342.12	Near Blackfoot to Neeley
85	124	4387.28	9.90E+04	4347.59	Near Blackfoot to Neeley
86	112	4353.76	9.90E+04	4313.88	Near Blackfoot to Neeley
86	113	4353.66	9.90E+04	4314.01	Near Blackfoot to Neeley
86	114	4353.66	9.90E+04	4314.18	Near Blackfoot to Neeley

Table 3 (contd.). List of model cells containing river cells representing the Snake River.

Row	Column	Stage (ft)	Riverbed Conductance (ft^2/day)	River Bottom Elevation (ft)	Reach
86	115	4353.66	9.90E+04	4314.27	Near Blackfoot to Neeley
86	116	4357.37	9.90E+04	4318.34	Near Blackfoot to Neeley
86	117	4359.68	9.90E+04	4320.81	Near Blackfoot to Neeley
86	118	4360.26	9.90E+04	4320.66	Near Blackfoot to Neeley
86	119	4363.43	9.90E+04	4323.18	Near Blackfoot to Neeley
86	120	4365.87	9.90E+04	4325.32	Near Blackfoot to Neeley
86	121	4373.64	9.90E+04	4332.18	Near Blackfoot to Neeley
87	111	4353.66	9.90E+04	4313.61	Near Blackfoot to Neeley
87	112	4353.76	9.90E+04	4313.88	Near Blackfoot to Neeley
87	113	4353.66	9.90E+04	4314.01	Near Blackfoot to Neeley
87	114	4353.66	9.90E+04	4314.18	Near Blackfoot to Neeley
88	107	4353.56	9.90E+04	4311.31	Near Blackfoot to Neeley
88	109	4353.67	9.90E+04	4313.3	Near Blackfoot to Neeley
88	110	4353.66	9.90E+04	4313.41	Near Blackfoot to Neeley
88	111	4353.66	9.90E+04	4313.61	Near Blackfoot to Neeley
88	112	4353.7	9.90E+04	4313.73	Near Blackfoot to Neeley
88	113	4353.66	9.90E+04	4314.01	Near Blackfoot to Neeley
88	114	4353.66	9.90E+04	4314.18	Near Blackfoot to Neeley
88	115	4353.66	9.90E+04	4314.18	Near Blackfoot to Neeley
89	106	4353.18	9.90E+04	4310.06	Near Blackfoot to Neeley
89	107	4353.56	9.90E+04	4311.31	Near Blackfoot to Neeley
89	108	4353.66	9.90E+04	4312.48	Near Blackfoot to Neeley
89	109	4353.67	9.90E+04	4313.3	Near Blackfoot to Neeley
89	110	4353.66	9.90E+04	4313.41	Near Blackfoot to Neeley
89	111	4353.66	9.90E+04	4313.61	Near Blackfoot to Neeley
89	112	4353.7	9.90E+04	4313.73	Near Blackfoot to Neeley
89	113	4353.66	9.90E+04	4314.01	Near Blackfoot to Neeley
89	114	4353.66	9.90E+04	4314.18	Near Blackfoot to Neeley
89	115	4353.66	9.90E+04	4314.18	Near Blackfoot to Neeley
90	104	4353.12	9.90E+04	4308.02	Near Blackfoot to Neeley
90	105	4352.87	9.90E+04	4308.82	Near Blackfoot to Neeley
90	106	4353.18	9.90E+04	4310.06	Near Blackfoot to Neeley
90	107	4353.56	9.90E+04	4311.31	Near Blackfoot to Neeley
90	108	4353.66	9.90E+04	4312.48	Near Blackfoot to Neeley
90	109	4353.67	9.90E+04	4313.16	Near Blackfoot to Neeley
90	110	4353.66	9.90E+04	4313.41	Near Blackfoot to Neeley
90	111	4353.66	9.90E+04	4313.61	Near Blackfoot to Neeley
90	112	4353.7	9.90E+04	4313.73	Near Blackfoot to Neeley
90	113	4353.66	9.90E+04	4314.01	Near Blackfoot to Neeley
90	114	4353.66	9.90E+04	4314.18	Near Blackfoot to Neeley
90	115	4353.66	9.90E+04	4314.18	Near Blackfoot to Neeley
91	103	4352.68	9.90E+04	4306.46	Near Blackfoot to Neeley
91	104	4353.12	9.90E+04	4308.02	Near Blackfoot to Neeley

Table 3 (contd.). List of model cells containing river cells representing the Snake River.

Row	Column	Stage (ft)	Riverbed Conductance (ft^2/day)	River Bottom Elevation (ft)	Reach
91	105	4353.29	9.90E+04	4308.74	Near Blackfoot to Neeley
91	106	4353.18	9.90E+04	4310.06	Near Blackfoot to Neeley
91	107	4353.56	9.90E+04	4311.31	Near Blackfoot to Neeley
91	108	4353.66	9.90E+04	4312.48	Near Blackfoot to Neeley
91	109	4353.67	9.90E+04	4313.16	Near Blackfoot to Neeley
91	110	4353.66	9.90E+04	4313.41	Near Blackfoot to Neeley
92	100	4348.82	9.90E+04	4299.47	Near Blackfoot to Neeley
92	101	4350.99	9.90E+04	4302.4	Near Blackfoot to Neeley
92	102	4352.79	9.90E+04	4305.13	Near Blackfoot to Neeley
92	103	4352.77	9.90E+04	4306.06	Near Blackfoot to Neeley
92	104	4353.12	9.90E+04	4308.02	Near Blackfoot to Neeley
92	105	4353.29	9.90E+04	4308.74	Near Blackfoot to Neeley
92	106	4353.18	9.90E+04	4310.06	Near Blackfoot to Neeley
92	107	4353.56	9.90E+04	4311.31	Near Blackfoot to Neeley
92	108	4353.66	9.90E+04	4312.48	Near Blackfoot to Neeley
92	109	4353.67	9.90E+04	4313.16	Near Blackfoot to Neeley
93	99	4327.91	9.90E+04	4277.3	Near Blackfoot to Neeley
93	100	4348.46	9.90E+04	4298.4	Near Blackfoot to Neeley
93	101	4350.99	9.90E+04	4302.4	Near Blackfoot to Neeley
93	102	4352.79	9.90E+04	4305.13	Near Blackfoot to Neeley
93	103	4352.77	9.90E+04	4306.06	Near Blackfoot to Neeley
94	99	4273.49	9.90E+04	4222.01	Near Blackfoot to Neeley
95	98	4240.65	9.90E+04	4188	Near Blackfoot to Neeley
95	99	4248.08	9.90E+04	4196.01	Near Blackfoot to Neeley
85	68	4172.75	3.51E+04	4123.2	Neeley to Minidoka
85	69	4190.45	3.51E+04	4140.28	Neeley to Minidoka
85	70	4192.86	3.51E+04	4141.68	Neeley to Minidoka
86	71	4195.25	3.51E+04	4142.87	Neeley to Minidoka
86	72	4195.28	3.51E+04	4141.95	Neeley to Minidoka
86	73	4195.02	3.51E+04	4141.09	Neeley to Minidoka
87	74	4195.44	3.51E+04	4140.29	Neeley to Minidoka
88	74	4196.01	3.51E+04	4140.01	Neeley to Minidoka
89	75	4195.99	3.51E+04	4138.93	Neeley to Minidoka
90	75	4196.08	3.51E+04	4138.09	Neeley to Minidoka
91	75	4195.54	3.51E+04	4136.65	Neeley to Minidoka
92	75	4195.62	3.51E+04	4135.82	Neeley to Minidoka
93	76	4196.07	3.51E+04	4134.87	Neeley to Minidoka
93	78	4196.18	3.51E+04	4133.16	Neeley to Minidoka
94	77	4195.92	3.51E+04	4132.94	Neeley to Minidoka
94	79	4196.18	3.51E+04	4133.16	Neeley to Minidoka
94	80	4196.18	3.51E+04	4133.49	Neeley to Minidoka
95	81	4196.18	3.51E+04	4134.13	Neeley to Minidoka
95	95	4196.6	3.51E+04	4140.24	Neeley to Minidoka

Table 3 (concluded). List of model cells containing river cells representing the Snake River.

Row	Column	Stage (ft)	Riverbed Conductance (ft^2/day)	River Bottom Elevation (ft)	Reach
95	96	4202.58	3.51E+04	4147.47	Neeley to Minidoka
95	97	4217.18	3.51E+04	4163.29	Neeley to Minidoka
96	82	4196.17	3.51E+04	4134.81	Neeley to Minidoka
96	83	4196.18	3.51E+04	4135.79	Neeley to Minidoka
96	90	4195.04	3.51E+04	4133.79	Neeley to Minidoka
96	93	4194.75	3.51E+04	4135.54	Neeley to Minidoka
96	94	4195.68	3.51E+04	4137.93	Neeley to Minidoka
97	84	4196.18	3.51E+04	4135.79	Neeley to Minidoka
97	85	4196.18	3.51E+04	4136.22	Neeley to Minidoka
97	86	4196.18	3.51E+04	4136.67	Neeley to Minidoka
97	87	4196.18	3.51E+04	4137.15	Neeley to Minidoka
97	88	4196.18	3.51E+04	4137.5	Neeley to Minidoka
97	89	4196.11	3.51E+04	4137.54	Neeley to Minidoka
97	91	4195.04	3.51E+04	4133.79	Neeley to Minidoka
97	92	4195.87	3.51E+04	4135.33	Neeley to Minidoka

Table 4. List of model cells containing drains representing springs in the Thousand Springs region.

Row	Column	Drain Elevation (ft) Elevation (ft)	Drain Conductance (ft^2/d)	Reach
70	30	3693.77	87.56523	Devils Washbowl to Buhl
69	29	3682	10.34861	Devils Washbowl to Buhl
68	29	3661	68.46006	Devils Washbowl to Buhl
66	28	3645.97	31711.91	Devils Washbowl to Buhl
65	28	3622.07	72169.5	Devils Washbowl to Buhl
65	27	3608.07	7904.277	Devils Washbowl to Buhl
64	26	3591	1273.676	Devils Washbowl to Buhl
62	24	3540.61	453546.3	Devils Washbowl to Buhl
61	23	3506	3502.608	Devils Washbowl to Buhl
59	22	3455	278.6165	Devils Washbowl to Buhl
58	21	3419.59	1512.49	Devils Washbowl to Buhl
57	20	3372	604.996	Devils Washbowl to Buhl
54	18	3250.03	941722.4	Devils Washbowl to Buhl
53	17	3241.2	103486.1	Devils Washbowl to Buhl
51	14	3180	254.8987	Buhl to Thousand Springs
50	13	3150.01	185533.5	Buhl to Thousand Springs
50	12	3128.01	456229.9	Buhl to Thousand Springs
49	11	3100.02	189105	Buhl to Thousand Springs
48	11	3100	1058810	Buhl to Thousand Springs
47	13	3128.27	149180.1	Buhl to Thousand Springs
47	12	3107.83	641034.8	Buhl to Thousand Springs
46	13	3115.92	179172.9	Buhl to Thousand Springs
46	12	3094.06	307529.7	Buhl to Thousand Springs
45	12	3075	404081.1	Thousand Springs
44	12	3059.08	15649154	Thousand Springs
43	12	3050	500578.1	Thousand Springs
42	12	3072.47	29734.38	Thousand Springs
42	13	3096.3	24060.39	Thousand Springs to Malad
41	13	3098.59	2168.47	Thousand Springs to Malad
40	13	3095.04	944.3784	Thousand Springs to Malad
39	14	3074.71	33836.27	Thousand Springs to Malad
38	14	3072.87	949.0182	Thousand Springs to Malad
37	14	3047	11480.96	Thousand Springs to Malad
37	13	3058	34838.79	Thousand Springs to Malad
36	14	3016	9501.488	Thousand Springs to Malad
36	16	3072.35	1118337	Malad
36	15	2998.77	1158866	Malad
35	14	3007	19541.74	Malad to Bancroft
34	14	2978.97	78008.92	Malad to Bancroft
33	14	2949.78	21851.87	Malad to Bancroft
32	14	2931.01	14574.1	Malad to Bancroft
31	14	2939.88	6660.319	Malad to Bancroft
31	13	2923.55	12483.49	Malad to Bancroft
30	13	2957.8	1236.11	Malad to Bancroft
25	6	2787	75081.41	Malad to Bancroft

Table 5. List of tributary basins.

Basin	Average Annual Tributary Valley Underflow for ESPAM Model (acre feet)	Average Annual Tributary Valley Underflow for ESPAM Model (ft^3)	Average Tributary Valley Underflow for ESPAM Model (ft^3/stress period)
American Falls	20,000	8.51E+08	4.25E+08
Big Lost River	48,000	2.09E+09	1.04E+09
Big Wood River	8,900	3.87E+08	1.93E+08
Birch Creek	69,000	3.02E+09	1.51E+09
Blackfoot River	12,000	5.03E+08	2.51E+08
Camas/Beaver Creeks	193,000	8.39E+09	4.20E+09
Clover Creek	8,900	3.87E+08	1.93E+08
Goose Creek	24,000	1.04E+09	5.22E+08
Henrys Fork	98,000	4.25E+09	2.13E+09
Lincoln/Ross Creeks	3,600	1.55E+08	7.73E+07
Little Lost River	138,000	5.99E+09	3.00E+09
Little Wood River	21,000	9.28E+08	4.64E+08
Medicine Lodge Creek	8,000	3.48E+08	1.74E+08
Palisades	6,200	2.71E+08	1.35E+08
Portneuf River	56,000	2.44E+09	1.22E+09
Raft River	75,000	3.25E+09	1.62E+09
Rexburg Bench	16,000	6.96E+08	3.48E+08
Rock Creek	45,000	1.97E+09	9.86E+08
Silver Creek	47,000	2.05E+09	1.02E+09
Teton River	2,700	1.16E+08	5.80E+07
Thorn Creek	5,300	2.32E+08	1.16E+08
Willow Creek	26,000	1.12E+09	5.61E+08

Table 6. List of perched non-Snake River reaches.

Reach	Acre Feet/Stress Period	Acre Feet/Year
Basin 31 Flood Control	1,929	3,857
Below Magic Reservoir	41,023	82,046
Big Lost River 1	7,279	14,557
Big Lost River 2	3,651	7,302
Big Lost River 3	4,511	9,022
Big Lost River 4	2,084	4,168
Big Lost River Flood Control	6,435	12,870
Big Wood River Below Gooding	3,493	6,985
Birch Creek	4,144	8,288
Birch Creek Hydropower Discharge	6,227	12,455
Camas Creek	13,827	27,654
Camas National Wildlife Refuge	3,712	7,425
Little Lost River	3,088	6,175
Little Lost River Flood Control	3,723	7,446
Little Wood River 1	2,436	4,873
Little Wood River 2	1,095	2,190
Little Wood River 3	1,699	3,397
Lone Tree Flood Control (Camas Creek)	3,079	6,157
Medicine Lodge Creek	16,202	32,404
Milner-Pickets (TFCC)	1,408	2,815
Mud Lake	4,514	9,028
Murtaugh Lake	1,675	3,351
Total	137,233	274,466

Table 7. List of canals represented with specified flux.

Canal Name
Northside Main
Northside Wilson Lake
Milner-Gooding
Aberdeen-Springfield
Northside Laterals above Rim

Table 8. Six-year average of measured lysimeter winter ET for Kimberly, Idaho.

Month	Average ET, mm/day	Average ET, ft/month
November	0.7	0.069
December	0.4	0.041
January	0.6	0.061
February	1.0	0.093

Table 9. Calculated Winter-Time ET Rates, Feet Per Month

Station	County	ID	Elev (ft)	Nov ET (ft)	Dec ET (ft)	Jan ET (ft)	Feb ET (ft)
Aberdeen Exp	Bingham	100010	4400	0.069	0.041	0.061	0.072
American Falls 3 NW	Power	100227	4320	0.069	0.041	0.061	0.075
Arco 3 SW	Butte	100375	5330	0.050	0.041	0.042	0.042
Ashton	Fremont	100470	5110	0.059	0.041	0.049	0.049
Blackfoot Fire Dept	Bingham	100915	4320	0.069	0.041	0.061	0.075
Bliss	Gooding	101002	3270	0.069	0.041	0.061	0.109
Burley FAA AP	Cassia	101303	4160	0.069	0.041	0.061	0.080
Dubois Exp	Clark	102707	5460	0.046	0.038	0.038	0.038
Fort Hall Indian Age	Bingham	103297	4500	0.069	0.041	0.061	0.069
Hamer 4 NW	Jefferson	103964	4800	0.069	0.041	0.060	0.060
Hazelton	Jerome	104140	3770	0.069	0.041	0.061	0.093
IF 16 SE	Bonneville	104456	5720	0.036	0.030	0.030	0.030
IF FAA AP	Bonneville	104457	4740	0.069	0.041	0.061	0.061
Jerome	Jerome	104670	3770	0.069	0.041	0.061	0.093
MacKay Ranger St	Custer	105462	5910	0.029	0.024	0.024	0.024
Minidoka Dam	Minidoka	105980	4210	0.069	0.041	0.061	0.079
Paul	Minidoka	106877	4150	0.069	0.041	0.061	0.080
Picabo	Blaine	107040	4880	0.068	0.041	0.057	0.057
Poc WB AP	Bannock	107211	4770	0.069	0.041	0.060	0.060
Richfield	Lincoln	107673	4310	0.069	0.041	0.061	0.075
Shoshone	Lincoln	108380	3970	0.069	0.041	0.061	0.086
St Anthony	Fremont	108022	4970	0.065	0.041	0.054	0.054

Table 10. Irrigation Entity Table

Entity ID	Entity Name	Irrigation Company(ies) Included in Entity
IESW01	A & B 1	A & B Irrigation District
IESW02	Aberdeen Springfield 1	Aberdeen Springfield Canal Co
IESW03	Arcadia 1	Arcadia Reservoir & Canal Co Ltd
IESW04	Bell Rapids 1	Bell Rapids Mutual Irrigation Co
IESW05	Big Lost River 3	Big Lost River Irrigation District
		Moore Water Users Association
		Darlington Land & Irrigation Co
IESW06	Big Spring 3	Banbury Pipe Company Inc
		Big Spring Water Users Assn
		Hagerman Water Users Association
IESW07	Big Wood 4	Justice Ditch Co
		Thorpe Ditch Co
		Big Wood Canal Company
		Mullins Canal & Reservoir Co
IESW08	Blaine 1	Blaine County Canal Co
IESW09	Burgess 5	Burgess Canal & Irrigating Co
		North Rigby Irrigation & Canal Co Inc
		Parks & Lewisville Irrigation Co Inc
		Rigby Canal & Irrigation Co
		Clark & Edwards Canal Company
IESW10	Burley 1	Burley Irrigation District
IESW11	Butte and Market 1	Butte & Market Lake Canal Co
IESW12	Canyon Creek 3	Enterprise Irrigation District
		Canyon Creek Lateral Ditch Assn
		Canyon Creek Canal Co Inc
IESW13	Consolidated Farmers 4	Roxana Canal Co
		Consolidated Farmers Canal Co Ltd
		Saurey-Sommer Ditch
		Island Ward Canal Co

Entity ID	Entity Name	Irrigation Company(ies) Included in Entity
IESW14	Corbett 4	Corbett Slough Ditch Company
		Eastern Idaho Water Co
		Little Butte Irrigation Co Ltd
		Younie Ditch Co
IESW15	Dewey 1	Dewey Canal Co
IESW16	Egin 2	Egin Bench Canals Inc
		St Anthony Union Canal Co
IESW17	Fall River 1	Fall River Irrigation Co
IESW18	Falls 3	Falls Irrigation District
		Warm Creek Irrigation Co
		Fort Hall Indian Reservation
IESW20	Harrison 5	Rudy Irrigation Canal Co Ltd
		Harrison Canal & Irrigation Co
		Kite And Nord Ditch
		Enterprise Canal Co Ltd
		Butler Island Canal Co
IESW21	Heise 1	Heise Canal
IESW22	Idaho 2	Snake River Valley Irrigation District
		Idaho Irrigation District
IESW23	Independent 6	Lowder Slough Canal Co
		West Labelle Irrigation Co Ltd
		Dilts Irrigation Company
		Ellis-Bramwell Ditch C0
		Independent Irrigation Co
		Labelle Irrigating Co
IESW24	Island 1	Island Irrigation Co
IESW25	Little Wood 2	Fish Creek Reservoir Company Inc
		Little Wood River Canal Co
IESW26	Long Island 1	Long Island Irrigation Co
IESW27	Milner 1	Milner Irrigation District
IESW28	Minidoka 1	Minidoka Irrigation District
		Owsley Canal Company
		Holley Water Users Assn
Entity ID	**Entity Name**	**Irrigation Company(ies) Included in Entity**
IESW29	Mud Lake 4	Level Canal Co Inc
		Mud Lake Water Users Inc
IESW30	New Sweden 7	Smith-Maxwell Ditch Co
		New Sweden Irrigation District
		Shattuck Irrigation Co.
		Stattuck Irrigation Co
		Long Island Canal Co
		Blackfoot Irrigation Co
		Woodville Canal Co
IESW31	North Fremont 1	North Fremont Canal Systems Inc
IESW32	North Side 4	King Hill Irrigation District
		North Side Canal Company Ltd
		American Falls Reservoir Dist #2
		Dba Bs Farms & Irrigation Co
IESW33	Osgood 4	Owners Mutual Irrigation Co
		Osgood Canal Co Inc

		H & W Water Users Association
		Bear Island Water Assn
IESW34	Peoples 8	Watson Slough Ditch And Irrigation Companies
		Peoples Canal & Irrigation Co
		Parsons Ditch Co
		Wearyrick Ditch Co
		Trego Ditch Co
		Danskin Ditch Company
		New Lavaside Ditch Company Limited
		Riverside Canal Co
IESW35	Progressive 2	Poplar Irrigation District
		Progressive Irrigation District
IESW36	Reid 6	Consolidated Feeder Canal Co
		Liberty Park Irrigation Co Inc
		Texas Slough Irrigating Canal Co
		Reid Canal Co
		Lenroot Canal Co
		Sunnydell Irrigation District

Entity ID	Entity Name	Irrigation Company(ies) Included in Entity
IESW37	Reno 1	Reno Ditch Company Inc
IESW38	Rexburg 1	Rexburg Irrigation Co C/O Keith Erikson
IESW39	Silky 2	Silky Lateral Ditch Water Users Assn
		Silky Irrigation District
IESW40	Southwest 2	Oakley Canal Co
		Southwest Irrigation District
IESW41	Twin Falls 1	Twin Falls Canal Co
IESW42	Twin Groves 6	Wilford Irrigation And Mfg Co
		Pioneer Ditch Co Ltd
		Twin Groves Irrigation & Manufacturing
		Salem Union Canal Co Ltd
		Farmers Friend Irrigation Co Ltd
		North Salem Agr & Mill Canal Inc
IESW43	Woodmansee Johnson 6	Woodmansee-Johnson Canal Company
		Teton Irrigation And Manufacturing Co
		Pincock Garner Ditch Association
		Pincock-Byington Ditch Co
		Wolf Ditch Company
		Teton Island Feeder Canal Co
IESW44	Jefferson 3	Jefferson Irrigation Co
		Producers Irrigation Co
		Monteview Canal Co Inc
		Monteview Canal Co Inc

Table 11. Sprinkler ratios used for interpolation between specific years.

ENTITY_ID	May-80	May-82	May-87	May-92	May-97	Oct-00
IEGW501	0.150	0.254	0.520	0.686	0.710	0.720
IEGW502	0.200	0.230	0.310	0.389	0.500	0.550
IEGW503	0.875	0.885	0.910	0.934	0.960	0.975
IEGW504	0.981	0.982	0.986	0.989	0.992	0.994
IEGW505	0.983	0.986	0.992	0.997	0.999	1.000
IEGW506	0.770	0.803	0.880	0.917	0.945	0.960
IEGW507	0.580	0.657	0.830	0.904	0.920	0.930
IEGW508	0.530	0.617	0.840	0.940	0.963	0.970
IEGW509	0.640	0.692	0.810	0.864	0.880	0.890
IEGW600	1.000	1.000	1.000	1.000	1.000	1.000
IESW000	0.333	0.373	0.499	0.555	0.610	0.634
IESW001	0.150	0.311	0.520	0.676	0.710	0.720
IESW002	0.825	0.847	0.900	0.919	0.930	0.936
IESW005	0.700	0.731	0.810	0.880	0.934	0.970
IESW007	0.147	0.165	0.215	0.239	0.263	0.276
IESW008	0.540	0.570	0.650	0.729	0.800	0.840
IESW009	0.015	0.050	0.130	0.185	0.220	0.250
IESW010	0.010	0.150	0.600	0.733	0.850	0.910
IESW011	0.440	0.467	0.530	0.560	0.590	0.610
IESW012	0.867	0.870	0.875	0.879	0.897	0.897
IESW014	0.210	0.286	0.450	0.545	0.640	0.700
IESW015	0.000	0.000	0.010	0.015	0.025	0.030
IESW016	0.050	0.136	0.750	0.808	0.860	0.890
IESW018	1.000	1.000	1.000	1.000	1.000	1.000
IESW019	1.000	1.000	1.000	1.000	1.000	1.000
IESW020	0.050	0.082	0.190	0.226	0.260	0.280
IESW022	0.250	0.384	0.650	0.763	0.850	0.900
IESW025	0.210	0.318	0.600	0.700	0.800	0.860
IESW027	0.000	0.000	0.230	0.307	0.360	0.380
IESW028	0.130	0.219	0.550	0.714	0.800	0.840
IESW029	0.035	0.068	0.150	0.240	0.320	0.420
IESW030	0.180	0.292	0.630	0.801	0.910	0.960
IESW031	0.950	0.961	0.980	0.998	1.000	1.000
IESW032	0.000	0.000	0.600	0.750	0.840	0.900
IESW033	0.970	0.976	0.990	0.996	1.000	1.000
IESW034	0.540	0.582	0.690	0.741	0.800	0.830
IESW035	0.020	0.056	0.190	0.278	0.360	0.410
IESW036	0.020	0.049	0.120	0.149	0.180	0.195
IESW037	0.145	0.229	0.420	0.608	1.000	1.000
IESW038	0.251	0.286	0.251	0.216	0.251	0.251
IESW039	0.270	0.296	0.270	0.243	0.270	0.270
IESW040	0.400	0.528	0.800	0.921	1.000	1.000
IESW041	0.000	0.017	0.120	0.188	0.250	0.285
IESW044	0.020	0.041	0.100	0.161	0.300	0.370
IESW051	0.000	0.000	0.000	0.000	0.040	0.070
IESW052	0.000	0.000	0.000	0.000	0.040	0.070

IESW053	0.530	0.560	0.610	0.630	0.645	0.660
IESW054	0.319	0.359	0.467	0.510	0.560	0.588
IESW055	0.000	0.007	0.026	0.041	0.059	0.072
IESW056	0.451	0.468	0.507	0.536	0.571	0.584
IESW057	0.648	0.676	0.767	0.813	0.813	0.813

Table 12. Measured Return Flow Sites.

Site #	Station #	Site Name	Location	
Henry's Fork River basin:				
1	13055300	Farmers Own Canal - Black Spring	Lat. 44 02'59"	Long. 111 32'20"
2	13055337	Rexburg Canal drain nr Thornton	Lat. 43 48'55"	Long. 111 53'15"
3	13050543	Independent Canal drain		
4	13056550	Texas Slough Canal nr Thornton	Lat. 43 47' 58"	Long. 111 54' 49"
5	13056600	Texas Slough nr Rexburg	Lat. 43 47'17"	Long. 111 53'45.
6	13056650	Liberty Park Canal	Lat. 43 47'24"	Long. 111 55'27"
7	13056850	Bannock Jim Spring Slough	Lat. 43 46'30"	Long. 111 56'11"
Snake River to American Falls Reservoir:				
8	13057000	Scott's Slough	Lat. 42 44'32"	Long. 111 58'20"
9	13057020	Dry Bed	Lat. 43 42'11"	Long. 112 04'13"
10	13057030	South Parks	Lat. 43 41'19"	Long. 112 03'47"
11	13057045	Butte Market Lake Canal	Lat. 43 39'20"	Long. 112 05'27"
12	13057100	Burgess drain nr Idaho Falls	Lat. 43 36'60"	Long. 112 03'03"
Near to and just below American Falls Reservoir:				
13	13069548	Sterling Waste	Lat. 43 01'49"	Long. 112 43'40"
14	13069565	Aberdeen Waste Drain	Lat.	Long.
15	13076210	Tartar Waste	Lat. 42 52'40"	Long. 112 51'23"
16	13077650	Rock Creek nr American Falls	Lat. 42 39'10"	Long. 113 01'00"

Table 12 (continued). Measured Return Flow Sites.

Site #	Station #	Site Name	Location	
Below American Falls Reservoir to King Hill:				
17	13082060	F drain nr Declo	Lat. 42 32' 48"	Long. 113 37' 14"
18	13082032	D-3 drain	Lat. 42 36'49"	Long. 113 36'10"
19	13082062	D-5 drain nr Rupert	Lat. 42 33'15"	Long. 113 38'38"
20	13082064	D-4 drain nr Rupert	Lat. 42 34'15"	Long. 113 38'25"
21	13082320	Marsh Creek nr Declo	Lat. 42 31'26"	Long. 113 40'02"
22	13082330	Spring Creek nr Declo	Lat. 42 31'01"	Long. 113 41'03"
23	13084705	D-16 drain nr Heyburn	Lat. 42 32'30"	Long. 113 45'24"
24	13084707	B drain nr Heyburn	Lat. 42 33'33"	Long. 113 47'01"
25	13085060	D-17 drain nr Heyburn	Lat. 42 32'53"	Long. 113 50'51"
26	13085065	Main drain North nr Heyburn	Lat. 42 33'02"	Long. 113 51'59"
27	13085070	G drain nr Burley	Lat. 42 31'56"	Long. 113 53'12"
28	13085080	J drain nr Burley	Lat. 42 31'53"	Long. 113 53'29"
29	13089690	Irr drain nr Hansen	Lat.	Long.
30	13089695	Twin Falls Coulee	Lat. 42 34'11"	Long. 114 20'32"
31	13090370	Fish Hatchery Waste 0	Lat. 42 35'29"	Long. 114 26'03"
32	13090460	Perrine Coulee nr Twin Falls	Lat. 42 35'53"	Long. 114 28'20"
33	13091733	Jerome Golf Course Drain 1	Lat. 42 38 03"	Long. 114 31'03"
34	13093150	Sonnickson drain	Lat. 42 38'40"	Long. 114 33'26"
35	13093190	Sucker Flat drain nr Filer (LSLQ)	Lat. 42 38'25"	Long. 114 35'30"
36	13093550	Cedar Draw nr Filer	Lat. 42 39'13"	Long. 114 39'15"
37	13093900	Waste I nr Buhl	Lat. 42 39'33"	Long. 114 41'28"
38	13094050	J8 at Rivers Edge	Lat. 42 40'27"	Long. 114 44'27"
39	13094700	Mud Creek nr Buhl	Lat. 42 39'33"	Long. 114 47'20"
40	13095060	Fish Hatchery drain upper	Lat. 42 32'60"	Long. 114 49'21"
41	13095061	Fish Hatchery drain lower	Lat. 42 40'01"	Long. 114 48' 60
42	13095360	S. Coulee (Cedar Draw)	Lat. 42 41'46	Long. 114 48'19"
43	13095490	Irr Ditch to Blind Canyon	Lat. 42 42'28"	Long. 114 4730"
44	13133785	Drain nr Bickel Springs	Lat. 42 45'28"	Long. 114 50'48"
45	13152450	Irr Ditch nr Bliss	Lat. 42 55'56"	Long. 115 00'19"
46	13152895	W. drain nr Tuttle (Drain to Malad River)	Lat. 42 51'50"	Long. 114 51' 58"

Table 13. Assignment of return flows, diversions to surface water entities.

Below American Falls:

Group	Irr. Entity	Assigned Return flows		Water Supply: Historic Diversions	
1	IESW032	13152450	Irr. Ditch nr Bliss	13087000	T. F. Northside
		13152895	W. Dr. nr Tuttle (to Malad)	13086510	'A' Lateral in Gooding
		13133785	Drain nr Bickel Srings	13086520	N. Side Cross-cut
		13094050	J8 at Rivers Edge		
		13095490	Irr. Drain to Blind Canyon		
		13095360	S. Coulee(Ceder Draw)		
		13093150	Sonnickson drain		
		13091733	Jerome Golf drain		
2	IESW028	13085060	D-17 drain nr Heyburn	13080000	Minidoka Northside
		13085065	Main drain North nr Heyburn		
		13084707	B drain nr Heyburn		
		13084705	D-16 drain nr Heyburn		
		13082064	D-4 drain nr Rupert		
		13082062	D-5 drain nr Rupert		
		13082032	D-3 drain		
3	IESW010	13082060	F drain nr Declo	Minidoka South (13080500)	
		13082320	Marsh Creek nr Declo		
		13082330	Spring Creek nr Declo		
		13085070	G drain nr Burley		
		13085080	J drain nr Burley		
4	IESW041	13089690	Irr drain nr Hansen	13087500	Twin Falls Southside Canal
		13089695	Twin Falls Coulee		
		13090370	Fish Hatchery Waste 0		
		13090460	Perrine Coulee nr Twin Falls		
		13093190	Sucker Flat drain nr Filer (LSLQ)		
		13093550	Cedar Draw nr Filer		
		13093900	Waste I nr Buhl		
		13094700	Mud Creek nr Buhl		
		13095061	Fish Hatchery drain lower		
		13095060	Fish Hatchery drain upper		

Table 13(continued). Assignment of return flows, diversions to surface water entities.

Above American Falls

Group	Irr. Entity	Assigned Return flows	Water Supply: Historic Diversions
5	IESW002	13069548 Sterling Waste 13069565 Aberdeen Waste Drain 13076210 Tartar Waste	13061610 Aberdeen Springfield Canal
6	IESW031	13055300 Farmers Own Canal - Black Spring	13047575 Farmers Own 13047305 Yellowstone 13047415 Marysville
7	IESW016	13050543 Independent Canal drain (Ave. of 1989-90 USGS Data)	13049725 St Anthony Canal 13049550 Last Chance 13050525 Egin Canal 13050530 St Anthony Union Fdr 13050535 Independant Canal
8	IESW011	13057045 Butte Market Lake Canal	13057025 Butte Market Lake
9	IESW036	13056550 Texas Slough Canal nr Thornton 13056650 Liberty Park Canal 13056850 Bannock Jim Spring Slough 13056600 Texas Slough nr Rexburg	13038392 Sunnydell Canal 13038426 Lenroot Canal 13038431 Reid Canal 13038435 Bannock Jim 13038436 Hill Pitinger 13038437 Nelson Cory 13038434 Texas Feeder 13055323 Rexburg Canal 13055334 Rexburg Irr.

Table 13(concluded). Assignment of return flows, diversions to surface water entities.

Above American Falls

Group	Irr. Entity	Assigned Return flows		Water Supply: Historic Diversions
10	IESW009	13057000	Scott's Slough	13038110 Burgess
	IESW020	13057020	Dry Bed	13038115 Clark & Edwards
	IESW023	13057030	South Parks	13038180 Rigby Canal
	IESW024	13057100	Burgess drain nr Idaho Falls	13037975 Eagle Rock
	IESW026			13037977 Eagle Rock ab Will Cr
				13037985 Enterprise
				13038025 Butler Island
				13038030 Ross and Rand
				13038050 Steele Canal
				13038055 Harrison Canal
				13038065 Cheny Canal
				13038080 Butler Island #2
				13038095 Boomer Canal
				13038098 Kite & Nord
				13038145 Croft Pump
				13038387 Nelson Canal
				13038388 Mattson Creg
				1303838150 East Labelle
				13038205 Dilts Canal
				13038225 W. Labelle Long Is
				13038340 White Canal
				13038360 Bramwell
				13038362 Ellis Canal
				13038210 Island Canal

Table 14. Estimated return flow lags for the ten groups of surface irrigation entities.

Group	Irr. Entity	Results: Ann. Return and Lags					
1	IESW032	Total Annual Returned (%) =>		4.6			
		Month =>	1	2	3	4	5
		Lag. Ret. (%) =>	3	1.6	0	0	0
2	IESW028	Total Annual Returned (%) =>		4.80			
		Month =>	1	2	3	4	5
		Lag. Ret. (%) =>	2	1	1	1	0
3	IESW010	Total Annual Returned (%) =>		10.0			
		Month =>	1	2	3	4	5
		Lag. Ret. (%) =>	4	3	3	0	0
4	IESW041	Total Annual Returned (%) =>		6.4			
		Month =>	1	2	3	4	5
		Lag. Ret. (%) =>	3	2	1.5	0	0
5	IESW002	Total Annual Returned (%) =>		5.9			
		Month =>	1	2	3	4	5
		Lag. Ret. (%) =>	3	2	1	0	0
6	IESW031	Total Annual Returned (%) =>		19.5			
		Month =>	1	2	3	4	5
		Lag. Ret. (%) =>	7	4	3	3	2
7	IESW016	Total Annual Returned (%) =>		1.6			
		Month =>	1	2	3	4	5
		Lag. Ret. (%) =>	1	0.6	0	0	0
8	IESW011	Total Annual Returned (%) =>		1.8			
		Month =>	1	2	3	4	5
		Lag. Ret. (%) =>	1.8	0	0	0	0
9	IESW036	Total Annual Returned (%) =>		29.2			
	IESW038	Month =>	1	2	3	4	5
		Lag. Ret. (%) =>	12	10	5	2	1
10	IESW009	Total Annual Returned (%) =>		27.2			
	IESW020	Month =>	1	2	3	4	5
	IESW023	Lag. Ret. (%) =>	11	7	4	4	0
	IESW024						
	IESW026						

Table 15. Normalized annual Silver Creek flows.

Year	Annual (ac-ft)	Normalized Flux	Dampened Normalized Flux
1980/81	32383	1.17	1.06
1981/82	26539	0.96	0.99
1982/83	38543	1.39	1.13
1983/84	38628	1.39	1.13
1984/85	35633	1.29	1.1
1985/86	30812	1.11	1.04
1986/87	31684	1.14	1.05
1987/88	22700	0.82	0.94
1988/89	20691	0.75	0.92
1989/90	23278	0.84	0.95
1990/91	21075	0.76	0.92
1991/92	20976	0.76	0.92
1992/93	18595	0.67	0.89
1993/94	27301	0.99	1
1994/95	18327	0.66	0.89
1995/96	31272	1.13	1.04
1996/97	32242	1.16	1.05
1997/98	33892	1.22	1.07
1998/99	33167	1.2	1.07
1999/00	30072	1.09	1.03
2000/01	22677	0.82	0.94
2001/02	19090	0.69	0.9
Av Annual	27708	1	1

Table 16. Minor land use types.

Classification	Acres	Percent of Study Area	Recharge Rate
Dry Farm	95,000	1.3%	zero
Water and Wetlands	65,000	0.9%	Precipitation minus three feet/year
Cities and Industrial Areas	48,000	0.7%	Negative 1.2 feet/year

Table 17. Apportionment of Mud Lake fixed point pumpage.

Fixed Point	No. Wells	Adjusted No. Wells	Percent of Total Volume
Buck Springs	7	7	18%
Bybee	13	14	35%
Holley	6	8	21%
North Lake, East	12	7	18%
North Lake, West	3	3	8%

Table 18. Fixed point pumpage by stress period (ac-ft/stress period).

Stress Period	Snake/Teton Exchange Wells	Mud Lake Exchange Wells	Recharge Adjustment	Wetlands Adjustment
S1	-6,590	-76,926	0	-11,241
S2	0	-34,089	0	-5,294
S3	-13,082	-73,313	0	-11,241
S4	0	-17,936	0	-5,294
S5	-1,437	-57,902	0	-11,241
S6	0	0	0	-5,294
S7	-914	-23,598	0	-11,241
S8	0	0	0	-5,294
S9	-687	-15,563	0	-11,241
S10	0	0	0	-5,294
S11	-5,800	-69,008	0	-11,241
S12	0	0	0	-5,294
S13	-1,786	-60,730	0	-11,241
S14	0	0	0	-5,294
S15	-2,045	-112,847	0	-11,241
S16	0	0	417	-5,294
S17	-22,395	-167,982	12,933	-11,241
S18	0	-21,792	8,344	-5,294
S19	-7,379	-145,601	0	-11,241
S20	0	-42,358	0	-5,294
S21	-3,709	-159,949	626	-11,241
S22	-9,177	-52,773	8,344	-5,294
S23	-18,657	-145,528	12,725	-11,241
S24	-3,098	-40,742	8,344	-5,294
S25	-47,842	-163,418	30,246	-11,241
S26	0	-36,997	8,344	-5,294
S27	-998	-77,893	0	-11,241
S28	0	-49,972	0	-5,294
S29	-19,020	-156,706	0	-11,241
S30	0	0	0	-5,294
S31	-253	-34,435	0	-11,241
S32	0	-33,359	7,092	-5,294
S33	-448	-149,394	0	-11,241
S34	0	0	417	-5,294
S35	-103	-87,188	0	-11,241
S36	0	-14,917	1,669	-5,294
S37	-281	-52,254	0	-11,241
S38	0	0	0	-5,294
S39	-345	-62,114	0	-11,241
S40	0	0	0	-5,294
S41	-6,774	-166,460	0	-11,241
S42	-434	-43,060	0	-5,294
S43	-51,473	-175,595	37,963	-8,267
S44	0	0	12,308	-8,267
Average	-5,107	-59,600	3,404	-8,268
Annual Average	-10,215	-119,200	6,808	-16,535

Table 19. Evapotranspiration-indexed scale used to vary off-site pumping rates.

Year	Index	Year	Index
1980	0.94	1991	1.03
1981	0.98	1992	1.11
1982	0.97	1993	0.94
1983	0.96	1994	1.09
1984	0.94	1995	0.94
1985	1.01	1996	0.97
1986	1.03	1997	0.94
1987	1.07	1998	0.93
1988	1.10	1999	0.96
1989	1.03	2000	1.01

Table 20. Off-site well pumping for each model stress period (acre-ft per stress period).

Well ID	Location Name	S1	S2	S3	S4	S5	S6	S7	S8	S9	S10
1	Jefferson	-12,709	-410	-13,248	-405	-13,115	-401	-12,980	-393	-12,709	-422
2	Jefferson	-12,709	-410	-13,248	-405	-13,115	-401	-12,980	-393	-12,709	-422
3	Jefferson	-12,709	-410	-13,248	-405	-13,115	-401	-12,980	-393	-12,709	-422
4	Monteview	-6,338	-204	-6,609	-202	-6,540	-200	-6,474	-196	-6,338	-211
5	Monteview	-6,338	-204	-6,609	-202	-6,540	-200	-6,474	-196	-6,338	-211
6	Monteview	-6,338	-204	-6,609	-202	-6,540	-200	-6,474	-196	-6,338	-211
7	Producers	-1,479	-48	-1,542	-47	-1,526	-47	-1,510	-46	-1,479	-49
8	Producers	-1,479	-48	-1,542	-47	-1,526	-47	-1,510	-46	-1,479	-49

Well ID	Location Name	S11	S12	S13	S14	S15	S16	S17	S18	S19	S20
1	Jefferson	-13,655	-431	-13,926	-447	-14,465	-460	-14,874	-431	-13,926	-447
2	Jefferson	-13,655	-431	-13,926	-447	-14,465	-460	-14,874	-431	-13,926	-447
3	Jefferson	-13,655	-431	-13,926	-447	-14,465	-460	-14,874	-431	-13,926	-447
4	Monteview	-6,811	-215	-6,947	-223	-7,218	-229	-7,420	-215	-6,947	-223
5	Monteview	-6,811	-215	-6,947	-223	-7,218	-229	-7,420	-215	-6,947	-223
6	Monteview	-6,811	-215	-6,947	-223	-7,218	-229	-7,420	-215	-6,947	-223
7	Producers	-1,589	-50	-1,620	-52	-1,683	-54	-1,730	-50	-1,620	-52
8	Producers	-1,589	-50	-1,620	-52	-1,683	-54	-1,730	-50	-1,620	-52

Well ID	Location Name	S21	S22	S23	S24	S25	S26	S27	S28	S29	S30
1	Jefferson	-14,465	-431	-13,926	-464	-15,009	-393	-12,709	-456	-14,736	-393
2	Jefferson	-14,465	-431	-13,926	-464	-15,009	-393	-12,709	-456	-14,736	-393
3	Jefferson	-14,465	-431	-13,926	-464	-15,009	-393	-12,709	-456	-14,736	-393
4	Monteview	-7,218	-215	-6,947	-232	-7,484	-196	-6,338	-227	-7,353	-196
5	Monteview	-7,218	-215	-6,947	-232	-7,484	-196	-6,338	-227	-7,353	-196
6	Monteview	-7,218	-215	-6,947	-232	-7,484	-196	-6,338	-227	-7,353	-196
7	Producers	-1,683	-50	-1,620	-54	-1,746	-46	-1,479	-53	-1,715	-46
8	Producers	-1,683	-50	-1,620	-54	-1,746	-46	-1,479	-53	-1,715	-46

Well ID	Location Name	S31	S32	S33	S34	S35	S36	S37	S38	S39	S40
1	Jefferson	-12,709	-405	-13,115	-393	-12,709	-389	-12,573	-401	-12,980	-422
2	Jefferson	-12,709	-405	-13,115	-393	-12,709	-389	-12,573	-401	-12,980	-422
3	Jefferson	-12,709	-405	-13,115	-393	-12,709	-389	-12,573	-401	-12,980	-422
4	Monteview	-6,338	-202	-6,540	-196	-6,338	-194	-6,274	-200	-6,474	-211
5	Monteview	-6,338	-202	-6,540	-196	-6,338	-194	-6,274	-200	-6,474	-211
6	Monteview	-6,338	-202	-6,540	-196	-6,338	-194	-6,274	-200	-6,474	-211
7	Producers	-1,479	-47	-1,526	-46	-1,479	-45	-1,463	-47	-1,510	-49
8	Producers	-1,479	-47	-1,526	-46	-1,479	-45	-1,463	-47	-1,510	-49

Well ID	Location Name	S41	S42	S43	S44
1	Jefferson	-13,655	-464	-15,009	-418
2	Jefferson	-13,655	-464	-15,009	-418
3	Jefferson	-13,655	-464	-15,009	-418
4	Monteview	-6,811	-232	-7,484	-209
5	Monteview	-6,811	-232	-7,484	-209
6	Monteview	-6,811	-232	-7,484	-209
7	Producers	-1,589	-54	-1,746	-49
8	Producers	-1,589	-54	-1,746	-49

Table 21. Annual spring discharge (north side only) in the Milner to King Hill reach.

Water Year	Discharge (cfs)
1980	6110
1981	5860
1982	5760
1983	5690
1984	6030
1985	5830
1986	6350
1987	6260
1988	5960
1989	5820
1990	5610
1991	5460
1992	5190
1993	5090
1994	5320
1995	5120
1996	5040
1997	5430
1998	5870
1999	5660
2000	5830
2001	5870
2002	5440

Table 22. Estimated spring discharge by sub-reach in the Milner to King Hill reach.

Subreach Name	Number of Model Cells	Total Discharge (cfs)	Subreach Proportion of Milner to King Hill Discharge
Devil's Washbowl to Buhl Gage	17	1075	0.17
Buhl Gage to Thousand Springs	12	1700	0.28
Thousand Springs	4	1879	0.31
Billingsley Creek	10	204	0.03
Malad Gorge	2	1199	0.19
Malad Gorge to Bancroft Springs	10	97	0.02

Table 23. Model cells representing individually measured or estimated springs.

Spring	Row	Column
Devils Washbowl	66	28
Devils Corral	65	28
Blue Lakes	62	24
Crystal	54	18
Clear Lakes	50	12
	50	13
Briggs	49	11
Box	47	12
	47	13
Thousand Springs	44	12
Malad	36	15
	36	16

Table 24. Summary of spring discharge calibration target data.

Spring Name	Number of Observations	Start Date	End Date
Devils Washbowl	5657	4/6/85	9/30/00
Devils Corral	35	11/6/80	3/6/01
Blue Lakes	7470	5/1/80	9/15/02
Crystal	1802	6/3/85	2/18/02
Clear Lakes	56	10/13/82	1/16/02
Briggs	3462	5/19/80	9/30/98
Box	7458	5/1/80	9/30/00
Malad	217	12/1/84	12/1/02
Thousand Springs	236	5/1/80	12/1/02

Table 25. Steady state river gain and spring calibration targets and model predictions.

Spring or Reach Name	Steady State Target Discharge (ft^3/d)	Steady State Discharge (ft^3/d)
Ashton to Rexburg	2.72E+07	2.67E+07
Heise to Shelley	-5.14E+07	-5.19E+07
Shelley to Near Blackfoot	-6.43E+07	-6.35E+07
Near Blackfoot to Neeley	2.27E+08	2.28E+08
Neeley to Minidoka	7.08E+06	6.97E+06
Devils Washbowl to Buhl	8.66E+07	6.24E+07
Buhl to Thousand Springs	1.37E+08	1.32E+08
Thousand Ssprings	1.51E+08	1.70E+08
Thousand Springs to Malad	6.63E+06	5.34E+06
Malad	9.65E+07	1.04E+08
Malad to Bancroft	7.84E+06	1.14E+07

Table 26. Eastern Snake Plain Aquifer Model Enhancement Design Document Topics

Revised May, 2006

Model Design and Calibration	Author	ESPAM Project Document Number	IWRRI Document Number	Status
Model Design Objectives	Paul Castelin, Donna Cosgrove	DDM-001		Final
Model Boundary	Allan Wylie	DDM-002	IWRRI04-016	Final
Model Layers	Allan Wylie	DDM-003	IWRRI04-019	Final
Model River Representation	Allan Wylie	DDM-010	IWRRI04-017	Final
Estimating Elevation of Wellheads and River Surface	Allan Wylie	DDM-011	IWRRI04-021	Final
Delineating the Bottom of the Aquifer	Allan Wylie	DDM-012	IWRRI04-015	Final
Steady State Response Functions	Donna Cosgrove, Gary Johnson	DDM-013		In Preparation

Transient Response Functions	Donna Cosgrove, Gary Johnson	DDM-014		In Preparation
Model Grid and Grid Orientation	Allan Wylie	DDM-015	IWRRI04-018	Final
Confined vs. Unconfined Aquifer Representation	Allan Wylie	DDM-016	IWRRI04-020	Final
Estimating Reach Gains in the Ashton/Heise to Milner Reach	Brenda Gilliland	DDM-017	IWRRI04-011	Final
Estimating Reach Gains in the Milner to King Hill Reach	Gary Johnson	DDM-018		In Revision
ESPAM Final Report	Donna Cosgrove	DDM-019	IWRRI06-002	Final

Recharge Calculation	Author	ESPAM Project Document Number	IWRRI Document Number	Status
Determination of Crop Mix	Bryce Contor	DDW-001	IWRRI04-025	Final
Percolation, Runoff and Deficit Irrigation	Bryce Contor	DDW-002	IWRRI04-004	Final
Recharge from Precipitation on Non-Irrigated Lands	Bryce Contor	DDW-003	IWRRI04-006	Final
Tributary Underflow	Allan Wylie	DDW-004	IWRRI06-004	Final
Calculating Return Flow Lag Factors	Dick Lutz	DDW-005	N/A	Final
Aggregating Surface Water Canal Companies into Surface Water Irrigation Entities	Brenda Gilliland	DDW-008	IWRRI04-014	Final
Ground Water Irrigation Entities for Recharge Calculation	Bryce Contor	DDW-009	IWRRI04-026	Final
Traditional Evapotranspiration Calculation	Bryce Contor	DDW-010	IWRRI04-009	Final

PRISM Precipitation Maps	Brenda Gilliland	DDW-011	IWRRI04-013	Final
Estimating Irrigation Entity Diversions—Snake	Brenda Gilliland	DDW-012	IWRRI04-012	Final
Historical Gaging Station Locations	Brenda Gilliland	DDW-013	IWRRI04-022	Final
Historical Water Level Measurements	Suzy Shaub	DDW-014	Not assigned	Final
Land Use	Bryce Contor	DDW-015	IWRRI04-007	Final
Estimating ET Using SEBAL	Rick Allen	DDW-016		
Determining Source of Irrigation Water	Bryce Contor	DDW-017	IWRRI04-010	Final
Irrigation Conveyance Losses	Bryce Contor	DDW-020	IWRRI04-008	Final
ET Adjustment Factors	Bryce Contor	DDW-021	IWRRI06-005	Final
Discerning Method of Irrigation Water Application	Bryce Contor	DDW-022	IWRRI04-005	As-Built Version
Non-Snake Perched River Reach Seepage Estimates and Irrigation Diversions	Nathan Erickson	DDW-024	IWRRI06-003	Final

Fixed Point Pumping	Bryce Contor	DDW-026	IWRRI04-027	Final

Recharge Program	Author	ESPAM Project Document Number	IWRRI Document Number	Status
GIS-Based Recharge Program Component Design	Jim Oakleaf	DDR-001	N/A	Final (incorporated in Recharge Tool as help files)
Preparing GIS Recharge Component Inputs	Bryce Contor	DDR-002	N/A	Available as May, 2004 training notes
Fortran-Based Recharge Program Component User's Guide	Donna Cosgrove	DDR-003		In preparation

Field Work Reports	Author	ESPAM Project Document Number	IWRRI Document Number	Status
ADCP Reach Gain Measurement Report—Spring/Fall, 2001	Idaho Power/USGS	DDF-001	N/A	Final
ADCP Reach Gain Measurement Final Report	Idaho Power/USGS	DDF-005	N/A	Final
Return Flow Measurement Plan	Idaho Power	DDF-006	N/A	Final
Return Flow Measurement Data Report—Year 1	Idaho Power	DDF-007	N/A	Final
Return Flow Measurement Data Report—Year 2	Idaho Power	DDF-008	N/A	Final

Scenarios	Author	ESPAM Project Document Number	IWRRI Document Number	Status
Base Case Scenario	IWRRI	DDS-001	IWRRI04-001	Final
Curtailment Scenario	IWRRI	DDS-004	IWRRI04-023	Final
No Changes in Surface Water Practices Scenario	IWRRI	DDS-003	IWRRI04-003	Final
Managed Recharge Scenario	IWRRI	DDS-002	IWRRI04-002	Final
Drought Scenario	IWRRI	DDS-005	IWRRI04-024	In work
Strawman Scenario	IWRRI	DDS-006	IWRRI05-003	In Work
A&B Irrigation District Scenario	IWRRI	DDS-007		

Notes:
Web site for obtaining documents:
http://www.if.uidaho.edu/~johnson/ifiwrri/srpmrpts/index.html
DDM-nnn document number for model design documents
DDW-nnn document number for water budget design documents
DDR-nnn document number for recharge program design documents
DDF-nnn document number for field work design documents
DDF-nnn document number for scenario documents

MAPPING EVAPOTRANSPIRATION USING LANDSAT AND THE METRIC EVAPOTRANSPIRATION MODEL

Anthony Morse, **William J. Kramber**,
Idaho Department of Water Resources
PO Box 83720
Boise, ID 83720-00098
tony.morse@idwr.idaho.gov
bill.Kramber@idwr.idaho.gov

Richard G. Allen, **Masahiro Tasumi**
Department of Agricultural and Biological Engineering
Department of Civil Engineering
University of Idaho, Kimberly Research Station
Kimberly, ID 83341
rallen@kimberly.uidaho.edu
tasumi@kimberly.uidaho.edu

ABSTRACT

From 2000 to 2005, the Idaho Department of Water Resources and the University of Idaho used a NASA Synergy grant to develop an evapotranspiration model that uses Landsat TM data as the primary input. The METRIC evapotranspiration model computes a complete energy balance for each pixel from any satellite with visible, near infrared, and thermal infrared bands. Evapotranspiration is a component of the energy balance. The University of Idaho developed the METRIC model by modifying the European evapotranspiration model, SEBAL. The most significant modification is the incorporation of reference evapotranspiration as computed by the U.S. Bureau of Reclamation's system of AgriMet stations. The Idaho Department of Water Resources developed applications for METRIC in water planning, water rights monitoring, aquifer depletion, hydrologic modeling, water-use data, and water administration. The University of Idaho developed applications in California's Imperial Valley and in the Rio Grande Valley. Using Landsat data as input to the METRIC model has the advantages of a relatively small pixel size over large areal coverage at reasonable cost. Further, the archive of Landsat TM data allows mapping of evapotranspiration backwards in time for 20 years. The Idaho METRIC applications are one part of a rapidly expanding suite of world-wide applications for which the Landsat thermal band is critical.

INTRODUCTION

METRIC (Mapping Evapotranspiration at high Resolution and with Internalized Calibration) is an image-processing tool for computing evapotranspiration (ET). In METRIC, ET is a residual of the energy balance at the earth's surface. METRIC is a variation of the SEBAL, which was developed in the Netherlands by Bastiaanssen (1998a, 1998b). Unlike SEBAL, METRIC uses ground-based, reference ET. Both METRIC and SEBAL use Landsat Thematic Mapper data as the primary source of input data.

Initial application and testing of METRIC shows substantial promise as an efficient, accurate, and relatively inexpensive procedure to map actual ET from irrigated lands throughout a growing season. ET from satellite images may replace current procedures that rely on ground-based ET equations and generalized crop coefficients.

The internal calibration of the sensible heat computation within METRIC eliminates the need for atmospheric correction of reflectance measurements using radiative transfer models (Tasumi et al., 2004), and means that absolute temperature is not needed.

METRIC has been applied in several parts of the United States, but the bulk of the applications have been in Idaho, where the Idaho Department of Water Resources (IDWR) and the University of Idaho (UI) have used METRIC to compute monthly and seasonal ET for a variety of applications in water planning and water rights administration. IDWR has used METRIC to 1) set water budgets for hydrologic modeling, 2) monitor compliance with water rights, 3) support water planning, 4) estimate aquifer

depletion, and 5) estimate water use by irrigated agriculture (Allen, et al., 2005). UI has applied METRIC in other parts of the United States (Allen, et al., 2005).

THEORY

Allen, et al. (2005) explain the theory behind METRIC in detail, but Figure 1 offers a concise illustration. ET is calculated as a residual of the surface energy equation

$$LE = R_n - G - H$$

where LE is the latent energy consumed by ET, R_n is net radiation (sum of all incoming and outgoing shortwave and longwave radiation at the surface), G is sensible heat flux conducted into the ground, and H is sensible heat flux convected into the air. R_n is computed from satellite-measured narrow-band reflectances and surface temperature; G is estimated from R_n, surface temperature, and a vegetation index; and H is estimated from surface temperature ranges, surface roughness, and wind speed using buoyancy corrections. The algorithms used in METRIC for R_n and G stem from those used in early SEBAL applications by Bastiaanssen et al. (1998a).

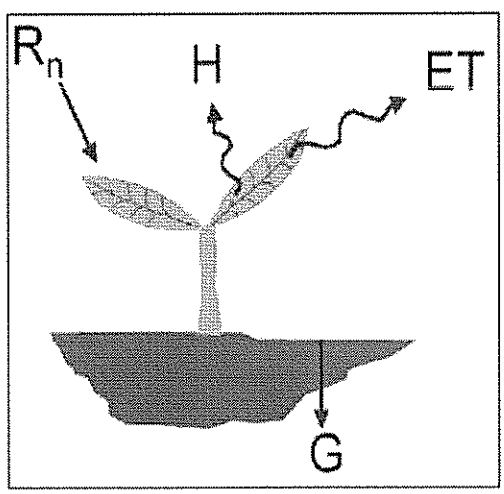

Figure 1. Diagram of the energy balance relationships that yield ET. R_n is net radiation, H is sensible heat convected to the air, G is sensible heat convected to the ground, and ET is evapotranspiration.

APPLICATIONS

IDWR developed five separate applications of the METRIC ET model. These applications use METRIC-derived ET to 1) set water budgets for hydrologic modeling, 2) monitor compliance with water rights, 3) compute ET by land use / land cover type, 4) compute aquifer depletion, and 5) compute water use by irrigated agriculture. UI applied METRIC to 1) examine ET patterns in agricultural fields, and 2) map ET from agriculture and riparian vegetation.

Water Budgets for Hydrologic Modeling

The Lower Boise Valley in Idaho is receiving significant attention because of rapid population growth. Beginning in 1995, IDWR led a multi-agency team in the construction of a groundwater model of the valley. The U.S. Bureau of Reclamation spent three years studying irrigation diversions from the Boise River and irrigation return flow into the river in order to better quantify the water balance for the model. The third main component of the water balance is ET.

IDWR compared METRIC-derived ET and the ET used in the 1996 Water Budget. This preliminary comparison was made using three model cells within the Treasure Valley Hydrologic Project ground water model; the selected cells were those three having the greatest flood-irrigated acreage. Each model cell is 2.59 km^2 in area.

Table 1 is an example of the data used in the initial comparison. The weighted average ET used in the 1996 Water Budget was 737 mm. This value was calculated using the ET crop coefficients for the 11 crop types, the percentage of total cropped area for each crop, and the average ET_r for the years 1988-1994 from the Parma Field Station. METRIC yielded more spatially variable ET values.

Model Row	Model Column	Hectares Flood Irrigated	Water Budget ET Millimeters	METRIC ET (1997) Millimeters
				Apr. 15 to Oct. 15
10	17	255	737	731
11	18	652	737	820
28	25	251	737	661

Table 1. A Comparison of METRIC ET with average ET for three cells of the Treasure Valley hydrologic model.

Monitoring Water Rights Compliance

IDWR presently has the technical means to identify diversions not having a water right by overlaying water-right polygons onto map-registered Landsat false-color images. However, the technical means to identify someone using water "in excess of the elements or conditions of a water right" is more problematic.

IDWR tested METRIC as an operational regulatory tool for administering water rights. The test attempted to identify fields onto which water was applied in violation of the maximum rate of diversion of the water right. The test covered part of the Eastern Snake River Plain, an area in Landsat path-row 39/30, for the 17-day period between and including two Landsat overpass dates. The test compared righted pumpage rates with ET for water-right places-of-use during the period of peak water demand in July. The comparison was done for 426 water rights in the study area, and compared cumulative ET, as computed by METRIC for the 17 days, with the maximum possible volume of water authorized to be diverted onto a field based on valid water rights.

UI/Kimberly personnel processed two July 2002 Landsat scenes (July 12 and July 28) through METRIC and delivered the data to IDWR. IDWR compared the ET data for the 426 fields with water rights data. The entire analysis was completed in less than 2 weeks after the second overpass date. Authorized diversion volume was calculated based on the allocated rate of flow, continuously diverted over the 17-day period. The comparison results are presented in Figure 2 where water right volume is plotted on the horizontal axis and consumption on the vertical axis. The points lying above the diagonal line indicate consumption exceeding authorized diversions. The line of points at 206 mm on the y-axis is a function of the bounds put on water rights by Idaho Statute.

IDWR personnel compared 426 water rights with METRIC-generated ET, and 18 of those were found to have ET greater than the water right could provide. Those 18 water rights were handed-off to water-rights personnel for further research.

The enforcement process using METRIC offers a significant improvement over the present method that uses power records. METRIC data can be processed for analysis during the irrigation season, which allows enforcement actions to be brought in a timely manner. Analysis of power meter records generally cannot be accomplished during the irrigation season due to the reporting protocols and restrictions on personnel time.

Evapotranspiration by Land Use/Land Cover Class

The purpose of this project was to compute the ET by land use/land cover (LULC) (Morse, et al., 2003). Water planners at IDWR need to understand how the demand for water will be affected during the next 50 years by the transition of land from irrigated agriculture to residential, commercial, and industrial LULC types. IDWR is responsible for comprehensive river basin planning in Idaho. One of the important issues the planners are contending with is the potential for water availability in a valley that is rapidly changing from agricultural land use to more urban types of land uses.

IDWR computed and mapped ET by LULC class. The U.S. Bureau of Reclamation and IDWR previously cooperated to generate an LULC classification of the Boise River Valley for the year 2000 from 1:24,000-scale aerial photographs. The classification consists of twenty-four LULC classes in a vector format.

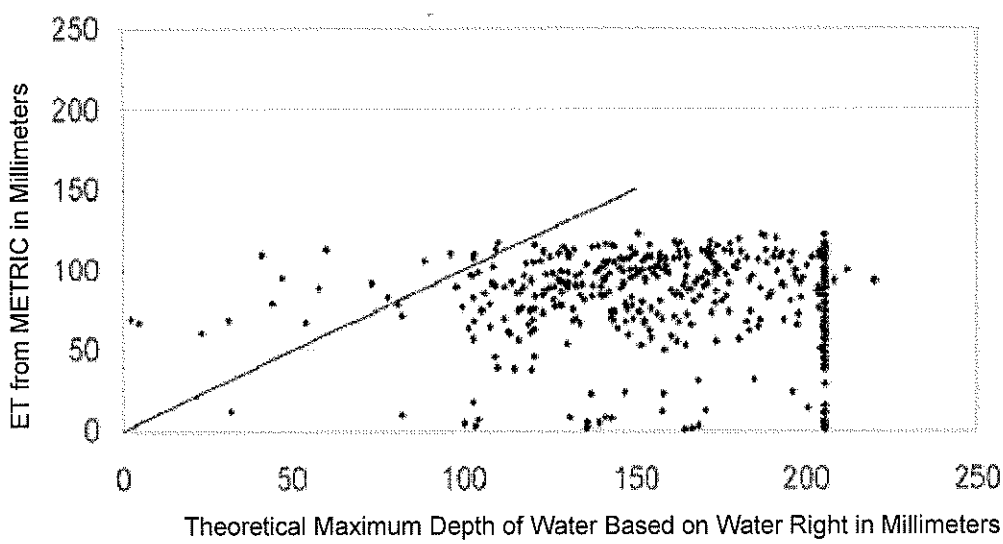

Figure 2. Comparison of cumulative METRIC ET with maximum water-right ET for 426 water right polygons in Idaho Department of Water Resources Basin 35 for July 12-July 28, 2002 period.

The aerial photographs were scanned to 1.5-meter pixels and registered to the Idaho Public Land Survey System base. The registered photographs were mosaicked into tiles that covered an area of approximately 93 square kilometers. IDWR personnel developed comprehensive descriptions of 24 LULC classes for the project. The descriptions were modified from MacConnell (1973) and are available in Kramber, et al., (1997).

For this analysis seven dates of Landsat data were processed through METRIC to develop seasonal ET for the period March 15 through October 15, 2000. The image dates are March 21, April 30, June 1, June 25, July 27, August 28, and October 2.

Figure 3a is a color infrared image of a portion of the lower Boise River Valley. Figure 3b is the corresponding area classified to land use and land cover. IDWR personnel overlaid the LULC polygons on the image of seasonal ET (Figure 3c) and computed the average seasonal ET for each class from all the polygons of each class. The result is summarized in Table 2, which shows the mean ET by LULC class with the associated standard deviation, and the total area of each class.

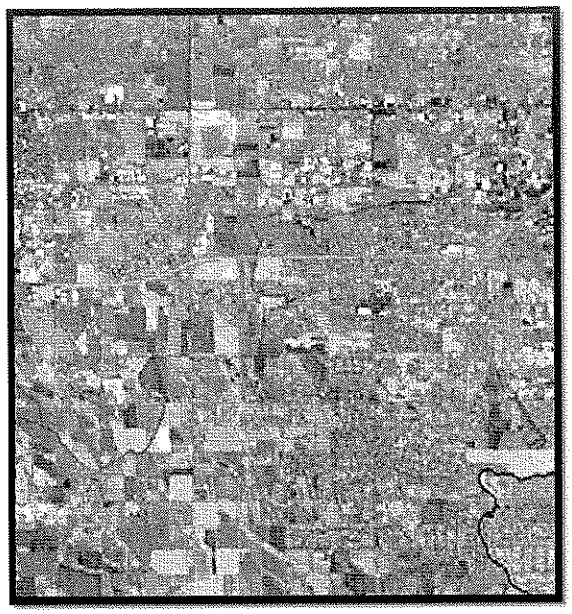

Figure 3a. FCC image of T3NR1E of the Boise Valley.

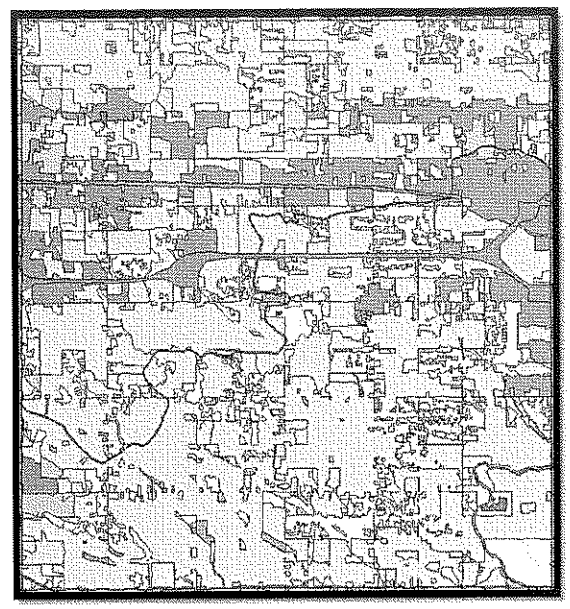

Figure 3b. Land use/land cover polygons in T3NR1E of the Boise Valley.

Figure 3c. ET image of T3NR1E the Boise Valley.

Class Name	Seasonal ET in mm	Standard Deviation	Area in hectares
Wetland	1,025	285	5,862
Water	924	165	5,344
Recreation	826	252	2,057
Perennial	820	212	2,711
Irrigated Crops	812	189	141,075
Canal	731	203	2,745
Urban Residential	684	157	4,126
Rural Residential	657	192	10,164
Farmstead	609	188	2,243
New Subdivision	606	146	11,516
Sewage	552	256	232
Public	548	263	2,120
Other Agriculture	536	243	2,853
Dairy	524	182	604
Feedlot	479	205	1,691
Junk Yard	467	193	129
Abandoned Agriculture	459	211	1,837
Transition	437	195	2,712
Idle Agriculture	436	215	3,042
Transportation	420	222	2,313
Commercial and Industrial	380	196	5,762
Barren	335	258	1,912
Unclassified	298	239	12,742
Rangeland	242	160	90,647
Petroleum Tanks	237	112	18

Table 2. Mean seasonal ET by land use/land cover class

Aquifer Depletion

The relationship between ET and ground water pumpage is important for IDWR regulatory processes. Historically, surface water diversions have been closely monitored while ground water diversions have not. Approximately 300 monitored diversions from the Snake River irrigate approximately 647,500 hectares on the Eastern Snake River Plain (ESRP). The ESRP also supports approximately 200,000 hectares of ground water irrigation from approximately 6,000 wells. From a logistical point alone, monitoring ground water pumpage is a large undertaking.

IDWR and other, associated organizations presently spend approximately $500,000 per year on monitoring ground water pumpage from the ESRP. The Water Distribution Section of IDWR has visited the 6,000 wells on the ESRP over the last 5 years to record the GPS location and to measure the well flow and simultaneous power consumption. These data are stored in the Water Management Information System, which is used to estimate ground water pumpage using the power-meter records for its constituent wells.

This application hypothesizes that there is a correlation between METRIC ET and ground water pumpage, and that for a given water right, the ET for the field or fields covered by that water right can be used to estimate the volume of water pumped from the corresponding well.

The comparison between METRIC ET and pumpage used 184 field-well combinations. Figure 4 shows the scatter plot of the two variables. No clear relationship is obvious, and a first-order polynomial regression confirms the lack of correlation with an $r^2 = 0.14$. Nevertheless, a close examination of the two data sets is revealing.

Figures 5a and 5b show the scatter within each individual variable of the dataset plotted with AgriMet ET data. The AgriMet data show the ET extremes of alfalfa and peas, and were recorded for the year 2000 at the U.S. Bureau of Reclamation AgiMet station in Aberdeen, Idaho. The Aberdeen Station is within approximately 32 km. of these fields, and is representative of them.

The two plots reveal useful information. In Figure 5a, nearly all the METRIC ET observations fall between the extremes of ET, which is the lowest at 365 mm for peas and highest at 890 mm for alfalfa. Further, there is a distinct "floor" at approximately 600 mm of ET, which is an indication of a practical minimum level of ET from irrigated agriculture. Most of the data fall well above peas, the local crop that uses the least water.

Contrast the METRIC ET pattern of Figure 5a with the pattern for pumpage as illustrated by Figure 5b. The pumpage data are not consistent at either the high end of the chart or at the low end. There is no "floor" evident to show that there is a minimum level of pumping needed to support an irrigated crop. In fact, the pumpage data set indicate that some fields are getting no water at all. The reliability of the dataset is called into question by the lack of patterns that reflect irrigation practice on the ESRP, and by the abundance of data at the extreme low end of the chart.

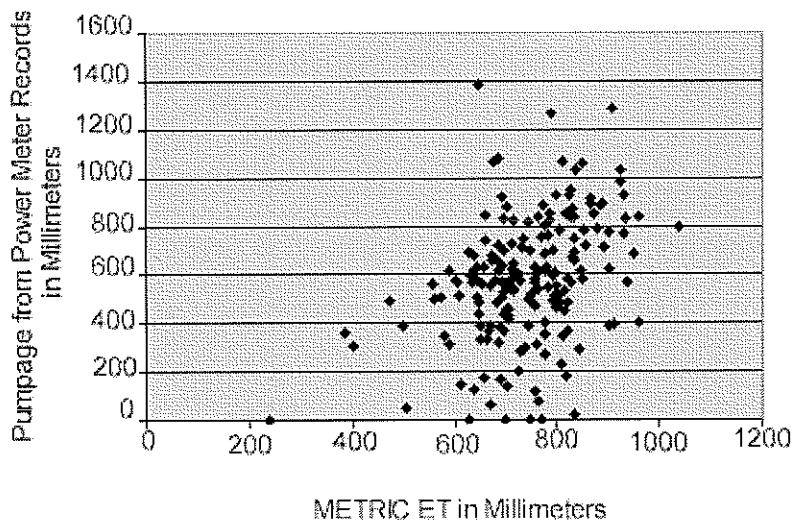

Figure 4. The scatter plot of pumpage versus METRIC ET in millimeters for the period April – October, 2000.

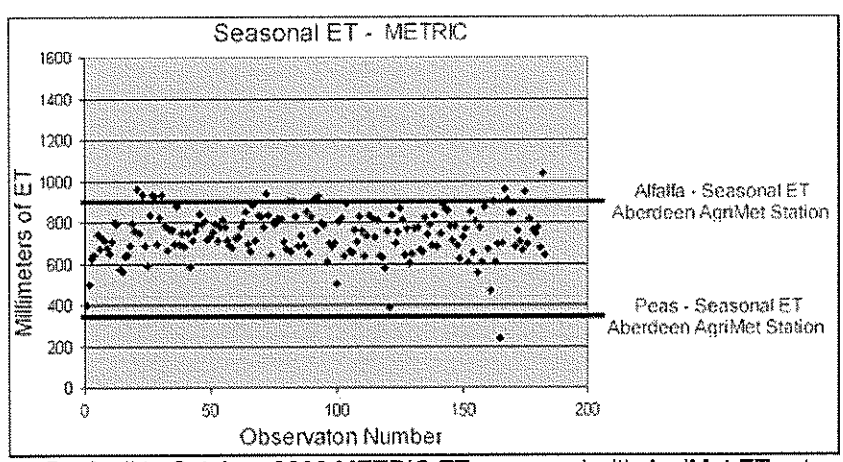

Figure 5a. April to October, 2000 METRIC ET compared with AgriMet ET extremes.

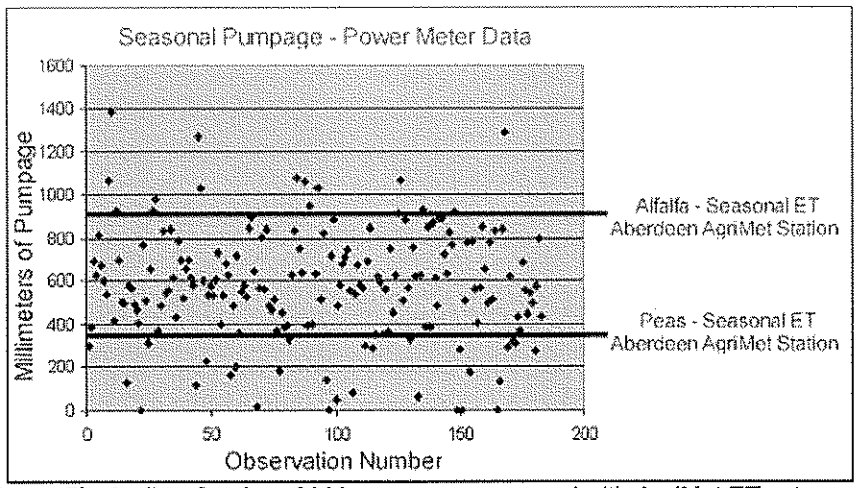

Figure 5b. April to October, 2000 pumpage compared with AgriMet ET extremes.

Water Use by Irrigated Agriculture

In 1995, the U.S. Geological Survey estimated consumptive water use by irrigated agriculture accounted for more than 99% of total water use in Idaho (Solley, et al., 1998). The most recent water-use estimate was done for the year 2000. Unlike previous years, USGS did not report water use by irrigated agriculture (Hutson, et al., 2004). The value of Idaho's irrigated agriculture was $2.58 billion in 1997. The Idaho Department of Water Resources wanted water use statistics for 2000, but knew the process would be expensive and time-consuming. Landsat data processed through METRIC offered an alternative solution (Morse, et al., 2004).

Landsats 7 and 5 were used for this application, with multiple dates processed for nine nominal scenes for the year 2000 in 28 counties of southern Idaho, the region of the state where irrigated agriculture is concentrated. Land in irrigated agriculture was delineated using National Land Cover Data, other data, and thresholding of evapotranspiration values. METRIC computed 9,313,503 acre feet of evapotranspiration from 3,552,174 irrigated acres, or 2.6 acre feet per acre. The irrigated acreage is biased high due to the generalizing affect of the land use/land cover data set. Nevertheless, the results suggest that past water use data may have under estimated consumptive use.

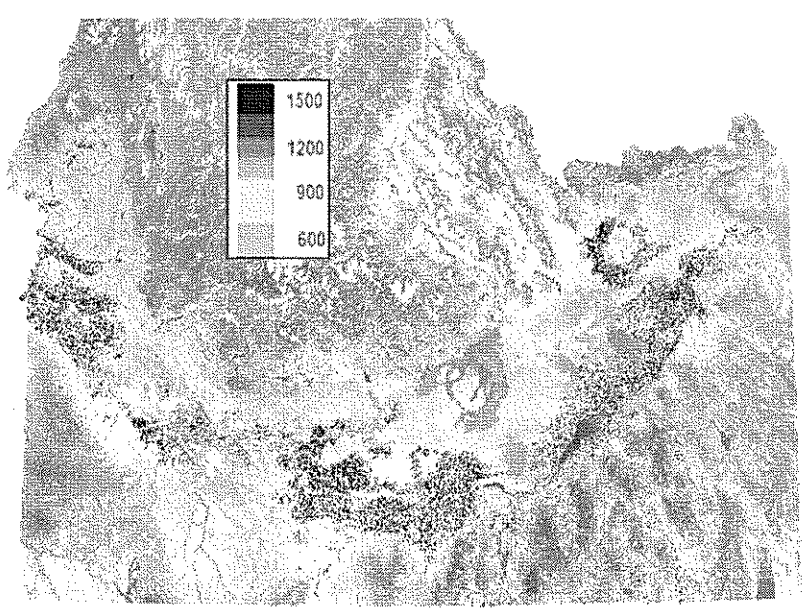

Figure 6. Agricultural ET in millimeters for southern Idaho developed from Landsat TM data. ET is seasonal (March 15, 2000 to October 15, 2000)

Applications in the Imperial Valley

Evapotranspiration maps have been created using METRIC and Landsat 7 images for much of Imperial Valley, California, for the January-March periods of 2002 and 2003 (Allen et al., 2003). The application demonstrated the ability to produce maps of quantitative, spatial distribution of monthly ET in near real time with resolution on the sub-field scale. The high resolution maps from Landsat were also useful in comparing ET in the "lower" ends of surface irrigated fields with ET in the "higher" ends of fields. Often, ET in lower ends of surface irrigated fields can suffer due to low irrigation uniformity or effects of salinity and inadequate leaching of salts.

Applications in the Middle Rio Grande

METRIC was applied with Landsat 5 and 7 images to irrigated and riparian areas along the Middle Rio Grande river of northern and central New Mexico for year 2002, to spatially and temporally quantify ET by irrigated crops and by riparian vegetation (native and invasive tree species and wetlands) (Allen et al., 2004). The high resolution of Landsat was, again, extremely valuable for assessing ET on a field by field basis and for estimating ET from riparian (tree) systems that were often less than 100 m in width. The Landsat based ET maps, derived for each month of the year, were valuable in showing the amount of evaporation from abandoned agricultural fields that had high water tables. The high water tables precluded farming operations and supplied water to the surface for evaporation. Reducing these evaporation losses by lowering water tables would constitute a real conservation of water in the valley.

REFERENCES

Allen, R.G. , A. Morse, M. Tasumi, W.J. Kramber, W. Bastiaanssen; 2005; Computing and Mapping of Evapotranspiration; Chapter 5 in Advances in Water Science Methodologies; U. Aswathanarayana, Ed.; A.A. Balkema Publishers; Leiden, The Netherlands

Allen, R.G., M.Tasumi and I. Lorite Torres; 2003; High Resolution Quantification of Evapotranspiration from Imperial Irrigation District. Research Completion report (phase I) submitted to MWD, December 2003. 130 p.

Allen, R.G., M. Tasumi, A. Morse, and R. Trezza; 2004; A Landsat-based Energy Balance and Evapotranspiration Model in Western US Water Rights Regulation and Planning. *J. of Irrig. and Drain. Sys;* vol 19, pp 251-268

Bastiaanssen, W.G.M., M. Menenti, R.A. Feddes, and A.A.M. Holtslag; 1998a; A remote sensing surface energy balance algorithm for land (SEBAL): 1. Formulation. *J. Hydrology,* 212-213, p. 198-212.

Bastiaanssen, W.G.M., M. Menenti, R.A. Feddes, and A.A.M. Holtslag; 1998b; The Surface Energy Balance Algorithm for Land (SEBAL): Part 2 validation, *J. Hydrology* , 212-213: 213-229

Hutson, S.S., N.L. Barber, J.F. Kinny, K.S. Linsey, D.S. Lumia, and M.A. Maupin; 2004; Estimated Use of Water in the United States in 2000; U.S. Geological Survey Circular 1268; U.S. Government Printing Office, Washington, D.C.

Kramber, W.J., A. Morse, B. Harmon, and H. Anderson; 1997; "Mapping 80 years of change in irrigated agriculture," Proceedings of the 1997 ACSM/ASPRS Annual Convention; Bethesda, MD, pp 367-372.

MacConnell, W.P.; 1973; Massachusetts Map-Down Publication 97, Cooperative Extension Service, University of Massachusetts.

Morse, A., W.J. Kramber, R.G. Allen, M. Tasumi; 2003; Preliminary Computation of Evapotranspiration by Land Cover Type Using Landsat TM Data and SEBAL; Proceedings of the 2003 International Geophysical and Remote Sensing Symposium; Toulouse, France

Morse, A., W.J. Kramber, R.G. Allen, M. Tasumi; 2004; Use of the METRIC Evapotranspiration Model to Compute Water Use by Irrigated Agriculture in Idaho; Proceedings of the 2004 International Geophysical and Remote Sensing Symposium; Anchorage, AK.

Solley, W. B., R. R. Pierce, and H.A. Perlman; 1998; Estimated Use of Water in the United States in 1995; U.S. Geological Survey Circular 1200, U.S. Government Printing Office, Washington, D.C.

Tasumi, M., R.G. Allen., R. Trezza, and J.L. Wright; 2005; Satellite-Based Energy Balance to Assess Within-Population Variance of Crop Coefficient Curves; ASCE J. Irrigation and Drainage Engineering; vol. 131, no. 1; pp 94-109

SATELLITE-BASED EVAPOTRANSPIRATION BY METRIC AND LANDSAT FOR WESTERN STATES WATER MANAGEMENT

Richard G. Allen[1], Masahiro Tasumi[1] and Anthony Morse[2]

[1]University of Idaho, Kimberly Research Center, Kimberly, ID 83341, USA
e-mail: rallen@kimberly.uidaho.edu; tasumi@kimberly.uidaho.edu
[2] Idaho Department of Water Resources, PO Box 83720, Boise, ID 83720-0098, USA e-mail: tony.morse@idwr.idaho.gov

Abstract

METRIC™ (Mapping Evapotranspiration at high Resolution and with Internalized Calibration) is an image-processing model comprised of multiple submodels for calculating evapotranspiration (ET) as a residual of the surface energy balance. METRIC is a variant of SEBAL, an energy balance process developed in the Netherlands by Bastiaanssen. METRIC was extended for application to mountainous terrain and to provide tighter integration with ground-based reference evapotranspiration. METRIC has been applied with Landsat images in southern Idaho, southern California, and New Mexico to predict monthly and seasonal ET for water rights accounting and for operation of ground water models. ET "maps" (i.e., images) via METRIC provide the means to quantify, in terms of both the amount and spatial distribution, the ET on a field by field basis. The ET images generated by METRIC show a progression of ET during the year as well as distribution in space.

Comparisons between ET by METRIC, ET measured by lysimeter and ET predicted using traditional methods have been made on a daily and monthly basis for a variety of crop types and land-uses. The results suggest that METRIC or similar methods hold substantial promise as efficient, accurate, and inexpensive procedures to predict the actual evaporation fluxes from irrigated lands throughout a growing season.

Introduction

Quantifying the consumption of water over large areas and within irrigated projects is important for water rights management, water resources planning and water regulation. Traditionally, ET from agricultural fields has been estimated by multiplying the weather-based reference ET by crop coefficients (K_c) determined according to the crop type and the crop growth stage. However, there is typically some question regarding whether the crops grown compare with the conditions represented by the K_c values, especially in water short areas. In addition, it is difficult to predict the correct crop growth stage dates for large populations of crops and fields. Recent developments in satellite remote sensing ET models have enabled us to accurately estimate ET and K_c for large populations of fields and water users and to quantify net ground-water pumpage in areas where water extraction from underground is not measured.

METRIC™ (Mapping Evapotranspiration at high Resolution and with Internalized Calibration) is an image-processing tool for calculating ET (Evapotranspiration) as a residual of the energy balance at the earth's surface. METRIC is a variant of the important model

SEBAL, an energy balance model developed in the Netherlands and applied worldwide by Bastiaanssen and his associates (1995, 1998a,b, 2000, 2005). METRIC has been extended to provide tighter integration with ground-based reference ET and has been applied with Landsat images to estimate monthly and seasonal ET for water rights accounting and for operation of ground water models.

METRIC and SEBAL represent a maturing technology for deriving a satellite-driven surface energy balance for estimating evapotranspiration (ET) from the earth's surface. This technology has the potential to become widely adopted and used by the world's water resources communities. ET maps created using METRIC, SEBAL or similar remote-sensing based processing systems will some day be routinely used as input to daily and monthly operational and planning models for reservoir operations, ground-water management, irrigation water supply planning, water rights regulation, and hydrologic studies.

The reasons why METRIC and SEBAL are attractive to western water resources management are:

- METRIC and SEBAL calculate *actual* ET rather than *potential* ET and do not require knowledge of crop type (no satellite-based crop classification is needed).
- METRIC and SEBAL rely heavily on theoretical and physical relationships, but provide for the introduction and automated calibration of empirical coefficients and relationships to make the process operational and accurate.
- The use of ET_r in calibration of METRIC and the use of ET_rF in extrapolation to 24-h ET provides general equivalency and congruency with ET as estimated using the traditional K_c ET_r approach, where ET_r is alfalfa reference ET calculated using the ASCE-EWRI standardized Penman-Monteith equation (ASCE-EWRI, 2004). This congruency is valuable for using ET maps generated by METRIC water rights management where water rights are based on previous K_c ET_r calculations.
- METRIC is auto-calibrated for each image using ground-based calculations of ET_r (made using weather data) where accuracy of the ET_r estimate has been established by lysimetric and other studies in which we have high confidence.

Internal calibration of the sensible heat computation within SEBAL and METRIC eliminates the need for atmospheric correction of T_s or reflectance (albedo) measurements using radiative transfer models (Tasumi et al., 2005a). The internal calibration also reduces impacts of any biases in estimation of aerodynamic stability correction or surface roughness.

The IDWR and the University of Idaho have developed a variety of METRIC applications. In Idaho, METRIC has been used to monitor water-right compliance and aquifer depletion, as a tool for water resource planning, and in hydrologic modeling (Morse et al., 2004). In the Rio Grande Valley of New Mexico, METRIC has been used to map ET from riparian vegetation. In the Imperial Valley of California, METRIC ET maps are used in irrigation management.

Theoretical Considerations

The theoretical and computational approaches of SEBAL and METRIC are described in Bastiaanssen et al., (1998a), Bastiaanssen (2000), Morse et al., (2000) and Tasumi et al. (2005b). Using an energy balance at the surface, energy consumed by the ET process is calculated as a residual of the surface energy equation:

$$LE = R_n - G - H \qquad (1)$$

where LE is the latent energy consumed by ET, R_n is net radiation (sum of all incoming and outgoing shortwave and longwave radiation at the surface), G is sensible heat flux conducted into the ground, and H is sensible heat flux convected into the air. The utility of using energy balance is that actual ET rather than potential ET (based on amount of vegetation) is computed so that reductions in ET caused by shortage of soil moisture are captured. Nevertheless, the computation of LE is only as accurate as are the values for R_n, G, and H. The algorithms used in METRIC for R_n and G are similar to those described for SEBAL by Bastiaanssen et al. (1998a) and the reader is referred to this and to Tasumi et al. (2005b) for detail. Basically, R_n is computed from satellite-measured broad-band reflectances and surface temperature; G is estimated from R_n, surface temperature, and vegetation indices; and H is estimated from surface temperature ranges, surface roughness, and wind speed using buoyancy corrections.

METRIC differs from previous applications of SEBAL principally in how the "H function" is calibrated for each specific satellite image. In both METRIC and SEBAL, H is predicted from an aerodynamic function where:

$$H = \rho C_p \frac{dT}{r_{ah}} \qquad (2)$$

where ρ is air density, C_p is specific heat of air at constant pressure, and r_{ah} is aerodynamic resistance between two near surface heights (generally 0.1 and 2 m) computed as a function of estimated aerodynamic roughness of the particular pixel and using wind speed extrapolated from some blending height above the ground surface (typically 100 to 200 m), with an iterative stability correction scheme based on the Monin-Obhukov functions (Allen et al.,1996). The dT parameter represents the near surface temperature difference between the two near surface heights. The dT parameter is used because of the difficulties in estimating surface temperature (T_S) accurately from satellite due to uncertainties in atmospheric attenuation and contamination and radiometric calibration of the sensor. In addition, T_s, as measured by satellite (i.e., radiometric temperature) can be several degrees different from "aerodynamic" temperature that drives the heat transfer process (Kustas et al., 1994, Norman et al., 1995, Qualls and Brutsaert, 1996). dT is designed to "float" above the surface, beyond the height for sensible heat roughness (z_{oh}) and zero plane displacement, and can be approximated as a relatively simple linear function of T_S:

$$dT = a + b\,T_s \qquad (3)$$

Bastiaanssen (1995), Bastiaanssen et al. (2005) and Allen et al., (2005a) provide rationale and empirical evidence for using the linear relation between dT and T_S. The application of equation (3) appears to extend well across a range of surface roughnesses, because as roughness increases and r_{ah} reduces, given the same H, dT reduces due to more efficient transfer of H, and T_S reduces for the same reason.

In traditional applications of SEBAL (Bastiaanssen et al. 1998a,b), parameters a and b in (3) are computed by setting dT = 0 when T_s is at the surface temperature of a local water body (or in its absence, a well vegetated field) where H is expected to be zero, and by setting $dT = (H\, r_{ah})/(\rho\, C_p)$ at T_s of a "hot" pixel that is dry enough so that one can assume that LE = 0. From (1) and (2), $dT = ((R_n\text{-}G)\, r_{ah})/(\rho\, C_p)$ at the "hot" calibration pixel. In METRIC, the same approach and assumptions are made for the hot pixel as in SEBAL, although a daily surface soil water balance is run for the hot pixel to confirm that ET = 0 or to supply a nonzero value for ET for the hot pixel for calibration of (3). For the lower calibration point of dT in METRIC, a well vegetated pixel having relatively cool temperature is selected and dT at that pixel is calculated as:

$$dT = \frac{(R_n - G - k\, ET_r)\, r_{ah}}{\rho\, C_p} \qquad (4)$$

where k is an empirical factor set to 1.05 because we assume that a viewed field having high vegetation and colder than average temperature, as compared to other highly vegetated fields, will have ET that is about 5% greater than ET_r due to higher surface wetness or merely due to its rank within the population of alfalfa fields (or other highly vegetated areas). The a and b coefficients are determined using the two values for dT paired with the associated values for T_s. With Landsat images, fields of alfalfa or other high leaf area vegetation can generally be identified that are close to or at full cover, so that the ET from these fields can be expected to be near the value of "reference ET" (ET_r) computed for an alfalfa reference. In METRIC, we use the standardized ASCE Penman-Monteith equation for alfalfa reference (ASCE-EWRI 2004), which is typically 20 to 30 percent greater than grass reference ET (ET_o). Generally, METRIC is applied without crop classification, so that specific crop type is generally not known.

METRIC and SEBAL, when applied with Landsat images, generally differ somewhat in how ET for the adjoining 24-h period is estimated given the essentially instantaneous ET calculated at the time of the satellite image (generally during late morning). In traditional applications of SEBAL, the evaporative fraction (EF), defined as the ratio of ET to (R_n-G), is assumed to be the same at both the observation time and for the 24-h period. The assumption of constant EF can sometimes underpredict 24-h ET in arid climates where afternoon advection or increases in afternoon wind speeds may increase ET in proportion to R_n (recent applications of SEBAL by SEBAL North America and WaterWatch, Inc. in arid settings have modified the 24-h EF to account for advection (Bastiaanssen, 2005, pers. commun.)). In METRIC, the extrapolation from observation time to the 24-h period is done using the fraction of reference ET (ET_rF) rather than EF. ET_rF is defined as the ratio of ET to ET_r (in the case of METRIC, ET_r is the alfalfa reference), and ET_rF is essentially the same as the well-known crop coefficient, K_c (for an alfalfa reference basis). The assumption of constant ET_rF during a day may be better able to capture impacts of advection and changing wind and humidity conditions during the day, as expressed in the ET_r calculation (which is done hourly and summed daily). Trezza (2002) and Romero (2004) demonstrated the general validity of constant ET_rF during a day using lysimeter data from Kimberly. Both METRIC and SEBAL continue to evolve as refinements to various components of the energy balance are made (Allen et al., 2005a,b).

Comparison with Measurements

ET measurements from precision, weighing lysimeters were compared against ET derived from METRIC using data from the Bear River Basin and from the USDA-ARS Kimberly Research Laboratory.

Lysimeters at Montpelier, Idaho

In Phase I (2000) of our study, ET maps were generated monthly for a 500 km x 150 km area (comprised of 2 Landsat images) encompassing the Bear River basin. Images were processed for 1985, coinciding with an ET study using lysimeters (Hill et al., 1989) that allowed for comparison to METRIC. Lysimeters near Montpelier, Idaho, just north of Bear Lake, had been planted to an irrigated native sedge forage crop characteristic of the area and local surroundings. The lysimeters were measured weekly. ET from the three lysimeters was averaged to reduce random error and uncertainty in the ET measurements. Results for four satellite images during the 1985 growing season (July 14, Aug. 15, Sept. 16, Oct. 18) are summarized in Figure 1 and Table 1. The results compare well to lysimeter data for the last three image dates. The earliest date, July 14, compares well when examined in context of the impact of precipitation preceding the image date and rapidly growing vegetation during that period (Morse et al., 2000). Daily ET on satellite image dates was calculated using EF, rather than ET_rF, in this early (year 2000) application. ET_rF generated from the daily METRIC application was used to interpolate between satellite images using daily ET_r. ET_r accounts for changes in ET caused by weather variation between satellite image dates. The predicted, monthly ET averaged +/- 16% relative to the lysimeter at Montpelier (Table 1). However, seasonal differences between METRIC and lysimeters were only 4% due to impacts of reduction in the random error components present in each estimate, such as random incidences of surface wetting by irrigation and in calculation of R_n, G, the dT function, and r_{ah}.

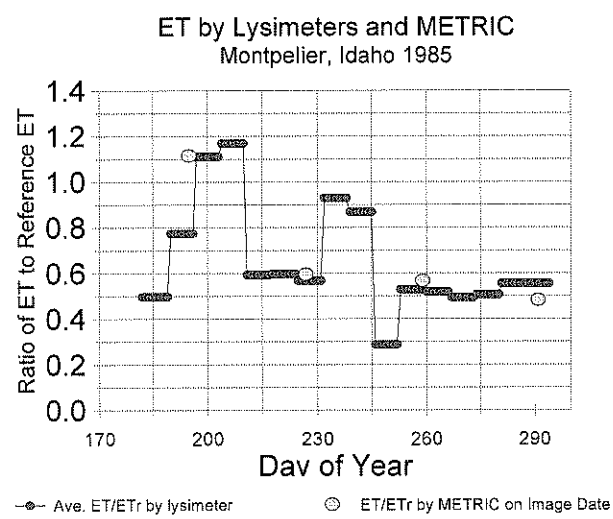

Figure 1. Comparison of ETr fractions (i.e., Kc) derived from 7-day lysimeter measurements near Montpelier, Idaho during 1985 and values from METRIC for four Landsat dates (ET = crop ET and ETr = alfalfa reference ET_r).

Lysimeters at Kimberly, Idaho

The validation of METRIC on the Snake River Plain has centered on the use of two precision-weighing lysimeter systems for ET measurement in place near Kimberly, Idaho, from 1968 to 1991. The lysimeter system was installed and operated by Dr. James Wright of the USDA-ARS (Wright, 1982, 1996) and measured ET fluxes continuously. ET data are available for a wide range of weather conditions, surface covers, and crop types. Measurements of net radiation, soil heat flux and plant canopy parameters were frequently made near the lysimeter site. The lysimeter data sets provided valuable information to verify METRIC over various time scales and for various conditions of ground cover.

Table 1. Summary of METRIC - and lysimeter-derived ET for weekly and monthly periods and the associated error for Bear River, 1985.

	7-day Lys. ET ave. surrounding image date (mm d^{-1})	METRIC ETrF on image date	7-day METRIC ET surrounding image date (mm d^{-1})	Diff. in 7-day ET (METRIC – Lys) (%	Monthly ET_r (mm)	METRIC Monthly ET (mm)	Lys. Monthly ET (mm)	Diff. in Monthly ET (METRIC – Lys.) (%)
(1)	(2)	(3)	(4)	(5)	(6)	(7)	(8)	(10)
July	5.3	1.12	6.8	28%	202	198	167	19%
Aug	3.5	0.59	3.7	6%	201	119	145	-18%
Sept	1.9	0.57	2.1	10%	115	66	54	22%
Oct	0.7	0.49	0.6	-14%	45	22	23	-5%
July-Oct.	2.9	0.73	3.3	15%	563	405	388	4%

Nineteen Landsat 5 satellite image dates were purchased for Kimberly, Idaho, covering the period between 1986 and 1991. These dates had quality lysimeter and cloud-free micrometeorological data and represent a combination of crop growth stages and times of the year. Eight images from 1989 are discussed here.

The lysimeter data for intervening periods between image dates were used to assess the impact of various methods for extending ET maps from a single day to longer periods. They have also been used to assess the variability in ET_rF over a day. The success of METRIC is predicated on the assumption that ET_rF for a 24-hour period can be predicted from the ET_rF from the instantaneous satellite image. ET_r was calculated for hourly and 24-hour periods using the ASCE standardized Penman-Monteith method for an alfalfa reference (ASCE-EWRI, 2004), representing the ET from a well-watered, fully vegetated crop, in this case, full-cover alfalfa 0.5 m in height. The denominator ET_r serves as an index representing the maximum energy available for evaporation. Weather data were measured near the lysimeter and included solar radiation, wind speed, air temperature and vapor pressure. An illustration of ET_rF for a day in 1989 is given in Figure 2 for clipped grass (*alta fescue*) and sugar beets. ET_rF for many days was even more uniform than shown in the figure. In nearly all cases, the ET_rF for the 24-hour period was within 5% of the ET_rF at 1030. Lysimeter data analyses showed $ET_rF = ET / ET_r$ to be preferable to the evaporative fraction (EF) parameter used in some applications of SEBAL (Bastiaanssen et al., 1998b, Bastiaanssen 2000)), where $EF = ET / (R_n - G)$. The

better performance by ET_rF was due to its consistency during daytime and agreement between hourly ET_rF at satellite overpass time (~1030) and daily average ET_rF. Figure 3a and b shows side-by-side comparisons of ET by the METRIC ET_rF procedure vs. lysimeter and ET by the EF method vs. lysimeter for satellite image dates, where the SEBAL application was of 2000 vintage and where 24-hour EF was assumed to equal EF at satellite overpass time.

Table 2 summarizes error between METRIC and lysimeter measurements during 1989, a year when a significant number (eight) of both lysimeter measurements of ET and Landsat images were available. Absolute error averaged 30% for the eight image days. When April 18 was omitted, the average absolute error was only 14%. April 18 was before planting of the sugar beets and represented a period of drying bare soil following precipitation. The field at this time was non-uniform in wetness due to differential drying, and differences between lysimeter and METRIC computation were only 1 mm. The standard deviation of error between METRIC and lysimeter for dates from May – September was 13%. In comparison, a commonly quoted standard error for ET prediction equations that are based on weather data, for example, Penman or Penman-Monteith-types of equations, is about 10% for daily estimates (Wright and Jensen 1978).

Table 2. Summary and computation of ET during periods represented by each satellite image and sums for April 1 – September 30, 1989, for Lysimeter 2 (Sugar Beets) at Kimberly, Idaho (lysimeter and weather data by Dr. J.L. Wright).

Image Date	Lys. ET on date (mm d^{-1})	METRIC ET on date (mm d^{-1})	Error on Image Date (%)	ET_r on date (mm d^{-1})	ET_r for period (mm)	Lys. ET summed daily for period (mm)	Lys. ET for period based on image date only (mm)	METRIC ET for period (mm)
(1)	(2)	(3)	(4)	(5)	(6)	(7)	(8)	(9)
4/18/89	0.73	1.74	139	6.78	147	28	16	38
5/4/89	6.61	5.09	-23	7.76	94	30	80	62
5/20/89	1.37	1.34	-2	7.27	90	22	17	17
6/5/89	1.73	1.78	3	6.68	118	24	30	31
6/21/89	2.39	2.54	6	6.33	127	62	48	51
7/7/89	7.96	5.89	-26	8.44	120	116	113	84
7/23/89	7.64	7.17	-6	7.38	253	266	262	246
9/25/89	5.51	7.40	34	8.00	201	171	138	186
4/1–9/30						718[a]	705[b]	714[c]
Percent	Error					--------	-1.8%	-0.6 %

[a]The sum of daily measurements computed as the sum over all days between Apr. 1 and Sept. 30.
[b]The sum of ET for each lysimeter period, computed by multiplying summed ET_r during the period by the ET_rF for the image date.
[c]The sum of ET by METRIC for the lysimeter field, computed by multiplying the summed ET_r during the period by the ET_rF computed on the image date by METRIC.

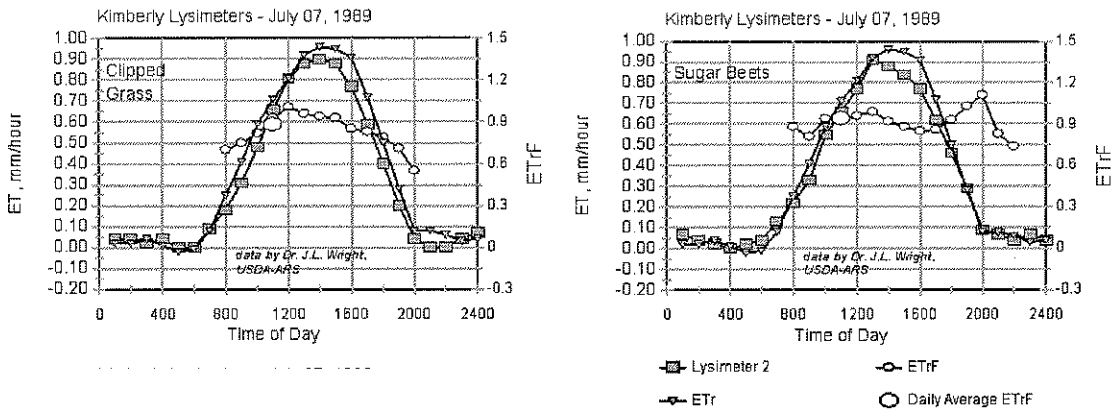

Figure 2. Hourly measurements of ET, ET_r, ET_rF, and 24-hour ET_rF for clipped grass (left) and sugar beets (right) at Kimberly Idaho on July 7, 1989.

The difference between METRIC (714 mm) and the lysimeter measurement (718 mm) was less than 1% for the growing season ET of the sugar beet crop. It appears that much of the error occurring on individual dates was randomly distributed, and tended to cancel, as described in more detail in Allen et al. (2005a). More recent applications of METRIC use linear interpolation of ET_rF between image dates and ET for periods is calculated by summing the product of ET_rF x ET_r on a daily basis (Allen et al., 2005b). Curvilinear interpolation of ET_rF over time can be used to follow typically convex shapes of ET_rF (i.e., K_c) curves that characterize annual vegetation. METRIC was able to obtain relatively good accuracy for the field surrounding the lysimeter. Results are illustrated in Figure 4, where ET is expressed in the form of ET_rF, which is used to normalize results for differences in climatic demand (i.e. ET_r). Round symbols and horizontal line segments represent ET_rF from lysimeter on the image date. These values are directly comparable with METRIC in Table 2. Triangular symbols represent ET_rF by METRIC for the image date.

Applications

Idaho Applications

Six separate applications and usage of the METRIC ET model and data have been made in Idaho to date by the Idaho Department of Water Resources (IDWR) and University of Idaho. These applications have been used: 1) to set water budgets for hydrologic modeling, 2) to monitor compliance with water rights, 3) to support water planning, 4) to estimate aquifer depletion, 5) to support ground-water modeling, and 6) to estimate water use by irrigated agriculture.

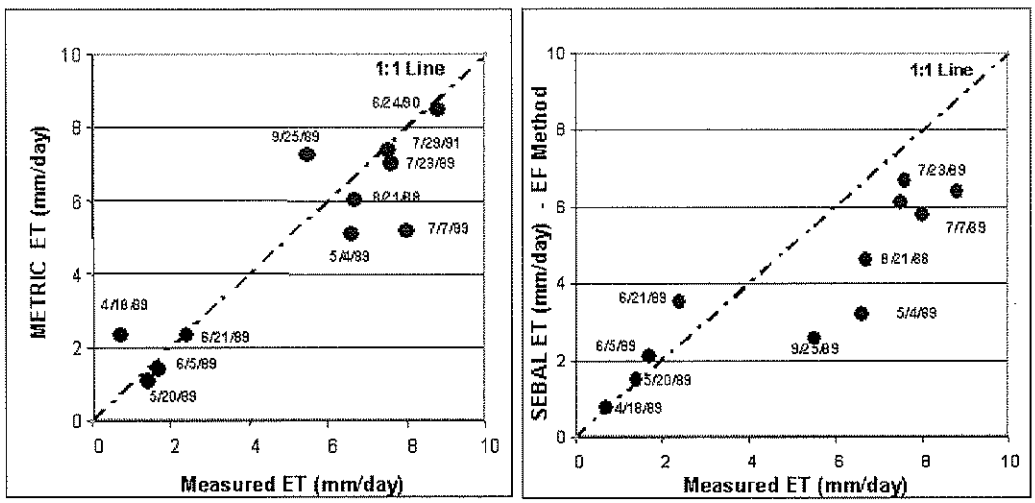

Figure 3. Comparison of daily ET using ET_rF (left) and EF (right) on satellite image dates for sugar beets (1989), potatoes (1988), peas (1990) and alfalfa (1991) (from Trezza, 2002).

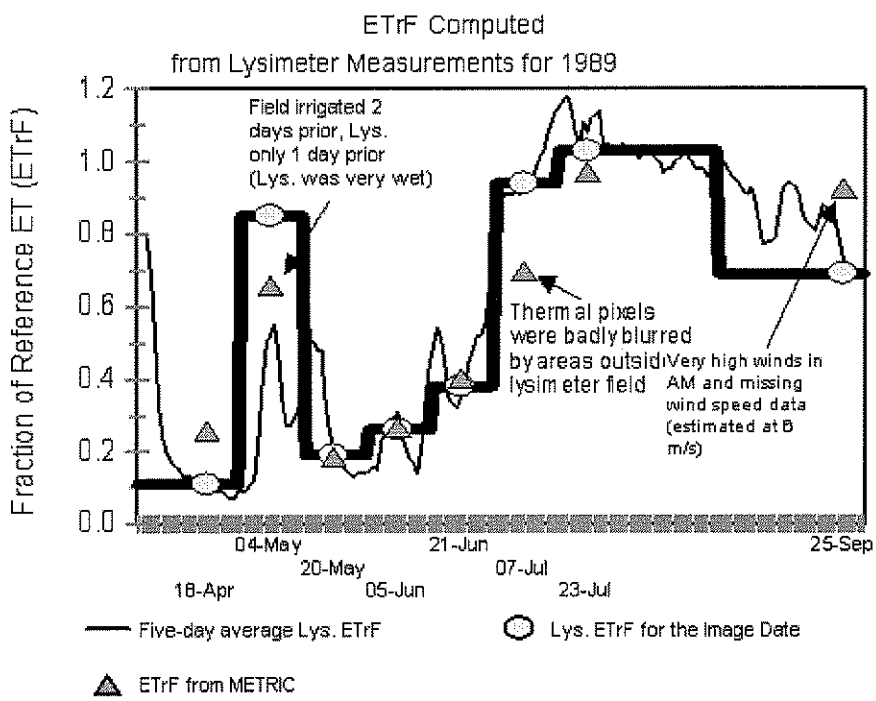

Figure 4. Results by METRIC and ET by Lysimeter as ET_rF. The thin line is the five-day average ET_rF for the lysimeter and the thick line is the period average ET_rF method used to extrapolate between images (as compared to linear and curvilinear methods currently used).

Water Budgets. Water budgets have been made of large portions of the lower Boise Valley in Idaho and eastern Snake Plain Aquifer in Idaho to improve accuracy of hydrologic models and projections. The Boise Vally has experienced rapid population growth and changing water consumption. The U.S. Bureau of Reclamation has spent the last three years studying irrigation diversions from the Boise River and irrigation return flow into the river in order to better quantify the water balance. The third main component of the water balance, ET, was quantified using monthly and annual ET maps derived from METRIC.

Water Rights. IDWR has tested and implemented a methodology to identify diversions not having a water right using water right place-of-use polygons and Landsat TM false-color composite data in GIS. However, the technical means to identify someone using water "in excess of the elements or conditions of a water right" is more problematic. IDWR has tested METRIC as an operational regulatory tool for administering water rights to identify those fields onto which water was applied in violation of some aspect of the water right, in this case the maximum rate of diversion. The 2002 test covered part of the Eastern Snake River Plain, an area in Landsat path-row 39/30. The test was a comparison of righted pumpage rates with ET for water-right places-of-use during the period of peak water demand in July. The comparison was done for 426 water rights in the study area and required comparing the righted pumpage rate and the minimum possible rate given the volume of ET from each associated water right place of use. The test utilized METRIC ET from 2 Landsat images taken 16 days apart and results were available to water rights analysts within 8 days of the second overpass. The enforcement process using METRIC was demonstrated to offer a significant improvement over the present method that uses power records. METRIC data can be processed for analysis during the irrigation season, which allows enforcement actions to be brought in a timely manner. Analysis of power meter records generally cannot be accomplished during the irrigation season due to the reporting protocols and restrictions on personnel time.

Water Planning. IDWR is responsible for comprehensive river basin planning in Idaho. One of the important issues planners are contending with is the potential for water availability in a valley that is rapidly changing from agricultural land use to more urban types of land uses. Water planners at IDWR need to understand how the demand for water will be affected during the next 50 years by the transition of land from irrigated agriculture to residential, commercial, and industry. The U.S. Bureau of Reclamation and IDWR have previously cooperated to generate a land-use/land-cover (LULC) classification of the Boise River Valley for the year 2000 from 1:24,000-scale aerial photographs. The classification consists of twenty-four LULC classes in a vector format. The availability of detailed LULC classes has enabled IDWR to combine the LULC classification with METRIC ET data to generate ET by land cover class. Preliminary values for ET by LULC class are summarized in Table 4 and illustrated in Figures 5-7.

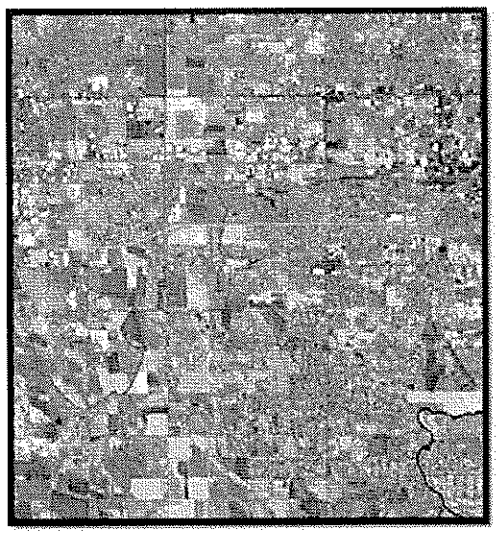

Figure 5. Color infrared image (aerial) of T3NR1E of the Boise Valley

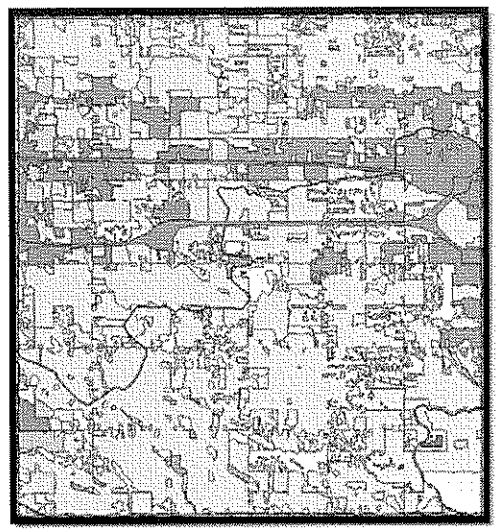

Figure 6. Land use/land cover polygons in T3NR1E of the Boise Valley

Figure 7. ET image of T3NR1E the Boise Valley (lighter intensity is higher ET)

Table 4. Ranked mean seasonal ET by land use/land cover class in the Boise Valley during 2000.

Class Name	Seasonal ET in mm	Standard Deviation	Area in hectares
Wetland	1,025	285	5,862
Water	924	165	5,344
Recreation	826	252	2,057
Perennial	820	212	2,711
Irrigated Crops	812	189	141,075
Canal	731	203	2,745
Urban Residential	684	157	4,126
Rural Residential	657	192	10,164
Farmstead	609	188	2,243
New Subdivision	606	146	11,516
Sewage	552	256	232
Public	548	263	2,120
Other Agriculture	536	243	2,853
Dairy	524	182	604
Feedlot	479	205	1,691
Junk Yard	467	193	129
Abandoned Agriculture	459	211	1,837
Transition	437	195	2,712
Idle Agriculture	436	215	3,042
Transportation	420	222	2,313
Commercial and Industrial	380	196	5,762
Barren	335	258	1,912
Unclassified	298	239	12,742
Rangeland	242	160	90,647
Petroleum Tank Yards	237	112	18

Aquifer Depletion and ground-water modeling. The Idaho Water Resources Research Institute (IWRRI) associated with the University of Idaho has recently recalibrated the MODFLOW ground-water model for the eastern Snake River Plain (ESRP) aquifer (and also for the Boise Valley aquifer). Spatial ET information derived from METRIC signficantly improved accuracy in distribution and quantity of depletions from the aquifer from pumping as well as improved estimates of incidental recharge to the aquifers from irrigation diversions from the Snake and Boise rivers.

Historically, surface water diversions have been closely monitored while ground water diversions have not. There are approximately 300 monitored diversions from the Snake River that irrigate approximately 647,500 hectares on the ESRP. The ESRP also supports

approximately 200,000 hectares of ground water irrigation, from approximately 5,000 wells. From a logistical point alone, monitoring ground water pumpage is a large undertaking.

For quantification of depletions by pumping, IDWR evaluated correlations between METRIC ET and ground water pumpage estimated using power consumption factor. The analysis evaluated ET from the field or fields covered by individual water rights as integrated from METRIC products and as recorded by power consumption for identified places of use (POU) in water rights. Pumpage estimates for 184 POUs vs. ET from METRIC are shown in Figure 8. While the r^2 for the relationship is only 0.14, some relation is evident. The relationship will shift leftward when corrected for effective precipitation that reduces pumping requirements. No adjustment for application efficiency was made. Some differences are due to pre- and post season irrigation by farmers to build soil moisture. Discussions within IDWR have placed more confidence in the METRIC results than in the pumping records for use in estimating net aquifer depletion due to questions concerning repeatability and consistency of power consumption factors. IDWR has estimated a 5:1 cost advantage of using METRIC and Landsat coverage to estimate ground-water depletions as compared to the current usage of power consumption factors that require occasional pump discharge measurements and system audits and reporting.

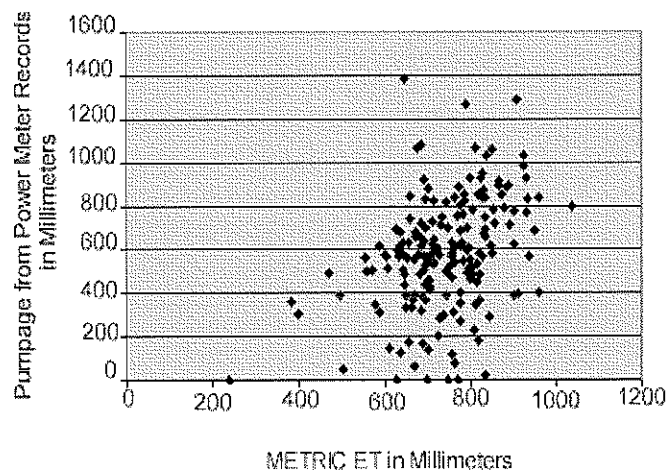

Figure 8. Ground-water pumpage from power consumption records versus METRIC ET in millimeters for the period April – October, 2000.

Applications in the Imperial Valley

Evapotranspiration maps have been created using METRIC and Landsat 7 images for much of Imperial Valley, California, for the January-March periods of 2002 and 2003 (Allen et al., 2003). The application demonstrated the ability to produce quantitative, spatial distribution of monthly ET in near real time with resolution on the sub-field scale. The high resolution maps from Landsat were useful in comparing ET in the "lower" ends of surface irrigated fields with ET in the "higher" ends of fields. Often, ET in lower ends of surface irrigated fields can suffer due to low irrigation uniformity or effects of salinity and inadequate leaching of salts.

Applications in the Middle Rio Grande

METRIC was applied with Landsat 5 and 7 images to irrigated and riparian areas along the Middle Rio Grande river of northern and central New Mexico for year 2002, to spatially and temporally quantify ET by irrigated crops and by riparian vegetation (native and invasive tree species and wetlands) (Figure 9). The high resolution of Landsat was valuable for assessing ET on a field by field basis and for estimating ET from riparian (tree) systems that were often less than 100 m in width. The Landsat based ET maps produced estimates of evaporation from abandoned agricultural fields in areas having high water tables (Figure 10). The high water tables precluded farming operations and supplied water to the surface for evaporation, where evaporation estimates for these areas exceeded natural precipitation (lower figure in 10). Reducing these evaporation losses by lowering water tables could conserve water in the valley.

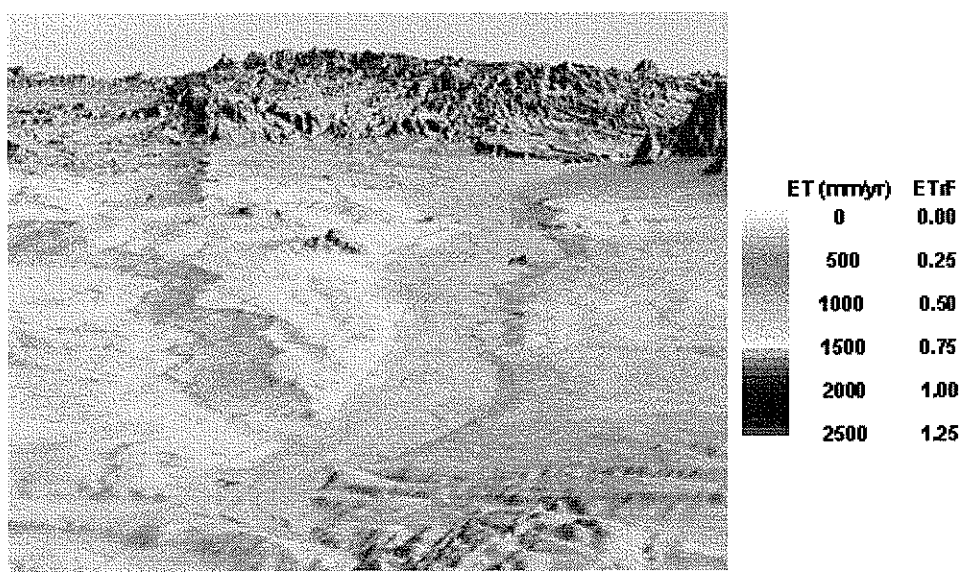

Figure 9. Pictorial of seasonal ET for 2002 for the Middle Rio Grande reach from San Acacia (just north of Socorro) north toward Colorado.

Figure 11 shows seasonal trends in ET_rF (i.e., K_c for an alfalfa reference) for eight randomly selected locations of cottonwood and salt cedar as classified by Neale (personal communication, 2004). The ET_rF for cottonwoods generally remained above 0.8 throughout the season, reflecting the tendency for cottonwood to populate areas having high water tables. Conversely, ET_rF for salt cedar ranged widely among the eight random locations, reflecting the impact on stand density and ET by wide ranges in water availability in areas populated by salt cedar. Figure 12 shows a frequency distribution of ET estimated for cottonwood and salt cedar during June and annually for 2002 for areas along the Middle Rio Grande from San Acacia to near Bernalilo. ET from salt cedar has larger variance due to its tendency to grow across a wider range of water availability (water table depth), soil types and salinity conditions. Monthly ET values and ET_rF for cottonwood, salt cedar, Russian olive and willow for the same area are listed in Table 5.

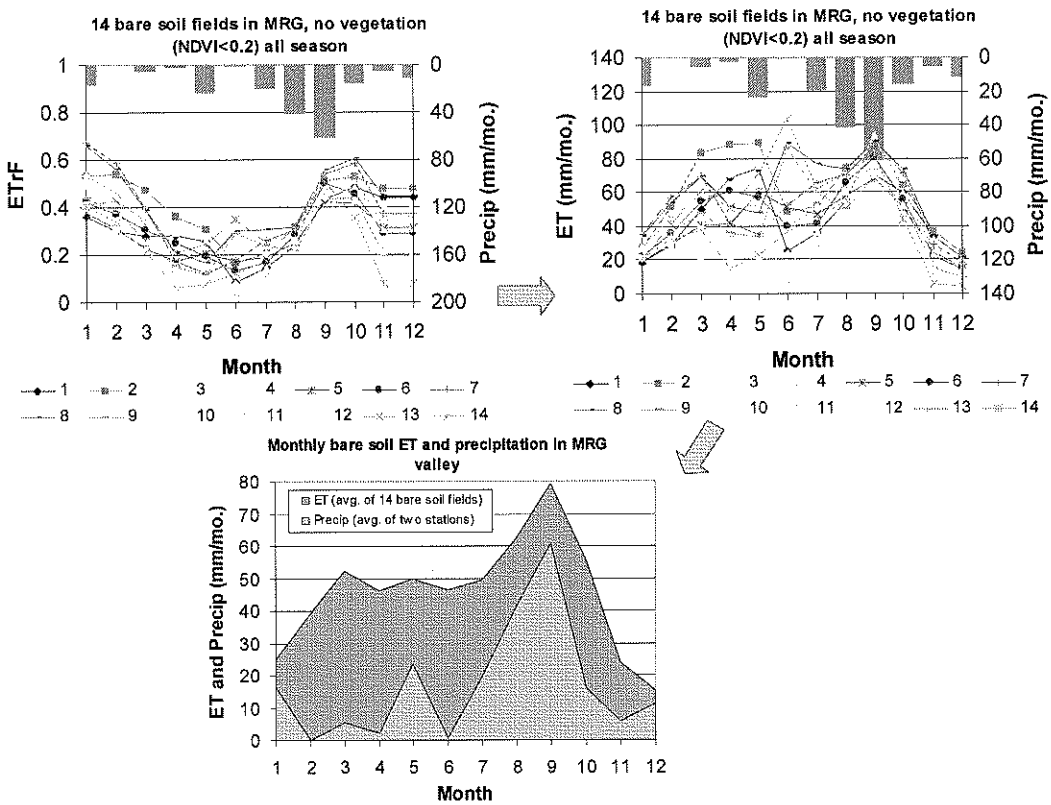

Figure 10. Evaporation during 2002 from areas having continuously bare soil along the MRG and precipitation received at Angostura and Boys Ranch (averaged).

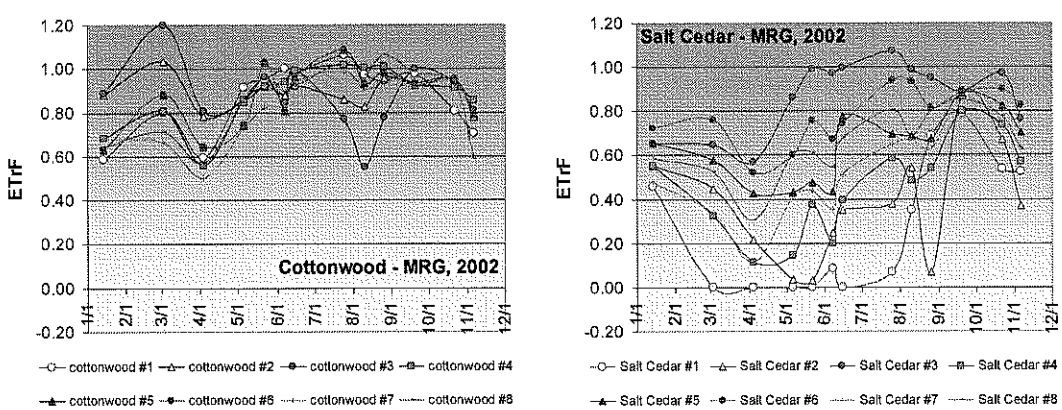

Figure 11. Seasonal trends in ET_rF (i.e., K_c for an alfalfa reference) for eight randomly selected locations of cottonwood and salt cedar along the MRG.

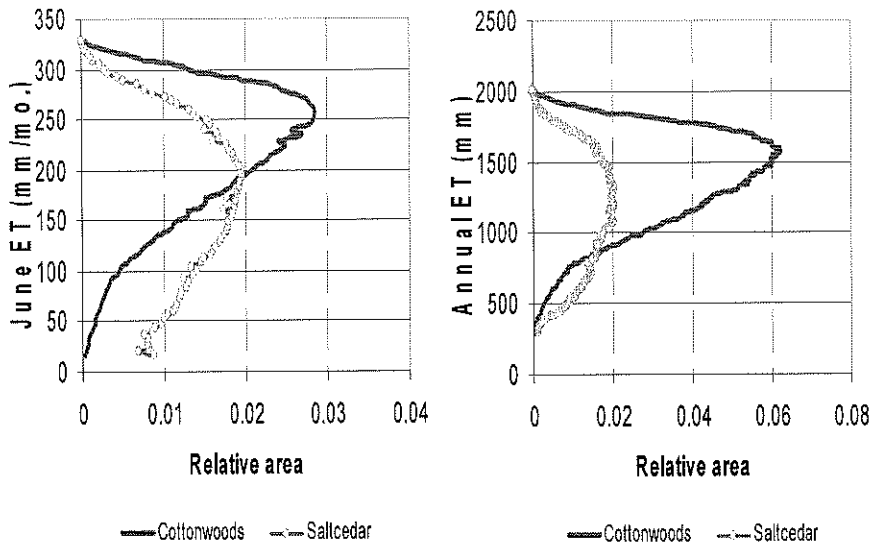

Figure 12. Estimated frequency distributions of ET from 6,000 ha of cottonwood and salt cedar along the MRG between Cochiti and San Acacia, NM during June and all of 2002.

Table 5. Monthly estimated water consumption by classes of riparian vegetation along the MRG area between Cochiti and San Acacia during 2002 and standard deviations (from Allen et al., 2004).

Month	ASCE-std ETr (mm/mo)	Cottonwood ET (mm/mo)	Cottonwood STDEV (mm/mo)	Saltcedar ET (mm/mo)	Saltcedar STDEV (mm/mo)	R.Olive ET (mm/mo)	R.Olive STDEV (mm/mo)	Willow ET (mm/mo)
1	52	30	6	28	7	31	6	30
2	96	51	18	43	21	52	21	47
3	178	84	35	65	39	88	40	75
4	243	123	47	91	52	130	47	110
5	290	183	60	130	70	192	56	165
6	296	215	58	155	75	226	61	196
7	249	198	47	154	61	207	52	180
8	232	186	35	155	44	194	37	173
9	161	134	16	125	18	140	15	133
10	122	98	12	93	15	102	14	96
11	77	48	10	45	14	50	11	47
12	48	30	6	28	9	31	7	30
Annual (mm)	2045	1380	307	1111	373	1442	332	1283

Month	Cottonwood ETrF	Cottonwood STDEV (ETrF)	Saltcedar ETrF	Saltcedar STDEV (ETrF)	R.Olive ETrF	R.Olive STDEV (ETrF)	Willow ETrF
1	0.58	0.11	0.54	0.14	0.59	0.12	0.57
2	0.53	0.18	0.44	0.22	0.54	0.22	0.49
3	0.47	0.20	0.36	0.22	0.49	0.22	0.42
4	0.51	0.19	0.37	0.21	0.54	0.19	0.45
5	0.63	0.21	0.45	0.24	0.66	0.19	0.57
6	0.73	0.20	0.52	0.25	0.76	0.21	0.66
7	0.79	0.19	0.62	0.24	0.83	0.21	0.72
8	0.80	0.15	0.67	0.19	0.83	0.16	0.74
9	0.83	0.10	0.77	0.11	0.87	0.09	0.83
10	0.80	0.10	0.76	0.12	0.83	0.11	0.79
11	0.63	0.13	0.59	0.18	0.65	0.14	0.62
12	0.62	0.13	0.59	0.18	0.65	0.15	0.61
Annual	0.67	0.15	0.54	0.18	0.71	0.16	0.63

Costs

ET data derived from METRIC are less expensive to generate for large areas than are standard ET data. Costs for monitoring water use on the eastern Snake River Plain are estimated to be about $500,000 per year. We estimate costs for remote sensing to be about $100,000 per year. This includes costs for 30 TM scenes representing 8 to 10 dates for the whole eastern Snake Plain (Landsat scenes cost about $400 each for images and about three Landsat images (160 km x 160 km) are required to cover the full area). Geo-registration of images costs an additional $400 each, for a total procurement cost of about $24,000. Once set up for an area, METRIC processing requires, on average, about 8 days per scene (240 days * 8 hours = 1920 hours * $40.00 per hour = $76,800 for processing for the full year for the full eastern Snake Plain). The total for remote sensing is therefore about $100,000. Set-up and time for aggregation of ET results via GIS results in a total remote sensing cost of $105,000. The estimated cost ratio of remote sensing to the current measurement program is $105,000/$500,000 = 0.21, i.e., remote sensing costs about 20% of the measurement costs. Measurement costs are for a subset of the total number of wells, all of which are not measured in a single year, whereas, METRIC data cover the entire Snake River Plain and all places of use. The use of METRIC ET will not replace the existing measurement program, per se. Pumpage data that can be related to individual water rights will be needed for regression against the METRIC ET data for the same water rights to establish the relationship between volume pumped and volume of ET. That relationship can then be applied to all other non-monitored water rights and their associated wells to estimate both aquifer depletion and water use by individual water rights.

Summary and Conclusions

METRIC and SEBAL use digital image data collected by Landsat and other remote-sensing satellites that record thermal infrared, visible and near-infrared radiation. ET is computed on a pixel-by-pixel basis for the instantaneous time of the satellite image. The process is based on a complete energy balance for each pixel, where ET is predicted from the residual amount of energy remaining from the classical energy balance, where ET = net radiation – heat to the soil – heat to the air.

In Phase 1 for the Bear River Basin and Phase 2 comparisons with precision weighing lysimeters at Kimberly, ID, differences between METRIC and the lysimeter for the growing season were less than 4%. These comparisons represent a small sample, but are probably typical. Errors as high as 10 to 20%, if distributed randomly, could probably be tolerated by IDWR and water user communities. Comparisons of METRIC ET with weighing lysimeter data at Kimberly, Idaho from the 1980's and early 1990's provided valuable information on the conditions required to obtain maximum accuracy with METRIC and best procedure for obtaining ET monthly and annually. ET was calculated for the entire Snake River Plain of SE Idaho and has improved the calibration of ground-water models by providing better information on ground-water recharge as a component of water balances. Ground-water pumpage from over 10,000 wells has been estimated using ET from METRIC through correlations between ET and pump discharge at measured wells and then extrapolating over large areas using ET maps from METRIC.

References

Allen, R.G. et al. (1996). "Evaporation and Transpiration." Chap. 4, p. 125-252 In: Wootton et al. (Ed.), *ASCE Handbook of Hydrology*. New York, NY.

Allen, R.G., M.Tasumi and I. Lorite Torres. (2003) *High Resolution Quantification of Evapotranspiration from Imperial Irrigation District.* Research Completion report (phase I) submitted to MWD, December 2003. 130 p.

Allen, R.G., M. Tasumi and C. Kelly. (2004). Middle Rio Grande Basin: METRIC™ ET Products and Description of Computational Processes. Final Report submitted to Keller-Bliesner Engineering, Logan, UT. University of Idaho Research and Extension Center, Kimberly, ID 83341. 39 p.

Allen, R.G., M. Tasumi, A. Morse, and R. Trezza. (2005a.) A Landsat-based Energy Balance and Evapotranspiration Model in Western US Water Rights Regulation and Planning. *J. of Irrig. and Drain. Sys.* (in press).

Allen, R.G., M. Tasumi and R. Trezza. (2005b). METRIC: Mapping Evapotranspiration at High Resolution – Aplications Manual for Landsat satellite imagery. University of Idaho. 130 p.

ASCE – EWRI. (2004). The ASCE Standardized reference evapotranspiration equation. ASCE-EWRI Standardization of Reference Evapotranspiration Task Comm. Report, available at http://www.kimberly.uidaho.edu/water/asceewri/

Bastiaanssen W.G.M. (1995) *Regionalization of surface flux densities and moisture indicators in composite terrain: A remote sensing approach under clear skies in Mediterranean climates.* Ph.D. Dis., CIP Data Koninklijke Bibliotheek, Den Haag, the Netherlands. 273 p.

Bastiaanssen, W.G.M., M. Menenti, R.A. Feddes, and A.A.M. Holtslag. (1998a.) A remote sensing surface energy balance algorithm for land (SEBAL): 1. Formulation. *J. Hydrology,* **212-213**, p. 198-212.

Bastiaanssen, W.G.M. et al. (1998b) The Surface Energy Balance Algorithm for Land (SEBAL): Part 2 validation, *J. Hydrology* , **212-213**: 213-229

Bastiaanssen, W.G.M. (2000) SEBAL-based sensible and latent heat fluxes in the irrigated Gediz Basin, Turkey. *J. Hydrology,* **229**:87-100.

Bastiaanssen W.G.M. et al. (2005) SEBAL for spatially distributed ET under actual management and growing conditions, *ASCE J. of Irrigation and Drainage Engineering* 131(1):85-93.

Hill, R.W., C.E. et al (1989) Duty of Water Under the Bear River Compact: Field Verification of Empirical Methods for Estimating Depletion. Research report 125. *Utah Agricultural Experiment Station*, Utah State University, Logan, Utah.

Kustas, W. P., et al., (1994). Surface energy balance estimates at local and regional scales using optical remote sensing from an aircraft platform and atmospheric data collected over semiarid rangelands. *Water Res. Research*, 30(5), 1241-1259.

Morse, A., M. Tasumi, R.G. Allen, W.J. Kramber (2000) *Application of the SEBAL Methodology for Estimating Consumptive Use of Water and Streamflow Depletion in the Bear River Basin of Idaho through Remote Sensing.* Synergy Phase 1 Final Report, IDWR, Boise, ID, 108 p.

A&B 2872

Morse, A., W.J. Kramber, R.G. Allen, and M. Tasumi (2004) *Use of the METRIC Evapotranspiration Model to Compute Water Use by Irrigated Agriculture in Idaho.* Proceedings of the 2004 IGARSS Symposium, Anchorage, AK.

Norman, J.M., W.P. Kustas, and K.S. Humes. (1995). Source approach for estimating soil and vegetation energy fluxes in observations of directional radiometric surface temperature. Ag. and For. Meteorology. 77:263-293.

Qualls, R., and Brutsaert, W. (1996). "Effect of vegetation density on the parameterization of scalar roughness to estimate spatially distributed sensible heat fluxes." *Water Resources Research*, 32(3), 645-652.

Romero M.G. (2004) *Daily evapotranspiration estimation by means of evaporative fraction and reference ET fraction.* Ph.D. Diss., Utah State Univ., Logan, Utah.

Tasumi M., Allen R.G., Trezza R. & Wright J.L. (2005a) Satellite-based energy balance to assess within-population variance of crop coefficient curves.. *ASCE J. Irrigation and Drainage Engineering.* 131(1):94-109.

Tasumi M., Trezza T., Allen R.G. & Wright, J.L. (2005b). Operational aspects of satellite-based energy balance models for irrigated crops in the semi-arid U.S. *J. of Irrig. and Drain. Sys.* (accepted).

Trezza R. (2002) *Evapotranspiration using a satellite-based surface energy balance with standardized ground control.* Ph.D. Diss., Utah State Univ., Logan, Utah.

Wright, J.L. (1982) New Evapotranspiration Crop Coefficients. *J. of Irrig. and Drain. Div.* (ASCE), 108:57-74.

Wright, J.L. (1996) Derivation of Alfalfa and Grass Reference Evapotranspiration. In *Evapotranspiration and Irrigation Scheduling,* C.R. Camp, E.J. Sadler, and R.E. Yoder (ed.). Proc. Int. Conf., ASAE, San Antonio, TX. p. 133-140.

Wright, J.L. and M.E. Jensen (1978). Development and evaluation of evapotranspiration models for irrigation scheduling. *Trans. ASAE* 21(1):88-96.